
Physics Research and Technology
Recent Developments in Dark Matter Research
Nori Kinjo • Akira Nakajima
Editors
NOVA
Complimentary Contributor Copy

in *Recent Developments in Dark Matter Research*. Editors: Nori Kinjo and Akira Nakajima
(Nova Science Publishers, Inc., 2013), pp. 1-61. ISBN: 978-1-62948-010-7
https://www.novapublishers.com/catalog/product_info.php?products_id=45466 DOI: 10.13140/2.1.5110.7841

Submicroscopic viewpoint on gravitation, cosmology, dark energy and dark matter, and the first data of inerton astronomy

Volodymyr Krasnoholovets

Indra Scientific, Square du Solbosch 26, B-1050, Brussels, Belgium

E-mail: v_kras@yahoo.com

Abstract

The so-called Standard Model of particle physics and the Standard Model of cosmology have so far not been able to suggest unambiguously what the very nature of dark matter is. These Models are therefore flawed at the fundamental level. We propose a deeper fundamental approach, the submicroscopic deterministic concept that considers the real space as a substrate constituted of primary topological balls arranging a tessellation lattice. Dark energy is accounted for by a peculiar distribution of topological balls inside the universe considered as a huge-range cluster in the total tessel-lattice. A moving particle interacts with the space generating spatial excitations named *inertons* by the author. Inertons being a substructure of the matter waves are present in any material object owing to the oscillating motion of its entities. Inertons form a vast series of harmonics that in the form of standing spherical waves spread far beyond the object inducing its Newton's gravitational potential. Starting from first submicroscopic principles the submicroscopic concept explained all phenomena predicted by general relativity. Dark matter is derived as a viscosity of space induced by standing inerton waves in the surrounding of star clusters. Two devices that measure inerton signals, which were designed by our team, are described. Some measurements of the Earth and Sun inerton signals conducted by using these devices are demonstrated. Finally we suggest designing the first inerton measuring complex, an inerton observatory, which will be able to measure amplitude, spectral and time characteristics of non-stationary inerton signals received from outer space.

1. Introduction

There are a number of review articles dedicated to the problem of dark matter (e.g. Garret and Dūda 2011). But the problem still looks as difficult for conventional cosmology and fundamental physics, as the notion of "dark matter" is not organically part of any of the main concepts. Researchers try to relate dark matter to massive objects in the universe rather

artificially, because this enigmatic substance cannot be derived directly from the main equations that currently describe the fundamentals of gravitational physics and cosmology. That is why, in order to understand and solve the problem of dark matter, we have to run through all three levels: descriptive, analytical and conceptual.

The descriptive level means astronomical observations and these are abundant: dark matter indeed was observed (Gilmore et al. 2007; Einasto 2010; Toffolatti et al. 2012; Benítez-Llambay et al. 2013).

The analytical level is represented by many diverse views, theories and experiments. Among major hypotheses we can name: MOND, which has actively been supported by a number of astronomers (Famaey and McGauph, 2012; 2013); cold dark matter (CDM) with the further broadening to the Lambda-CDM model, which includes CDM and parameterizes the Big Bang cosmological model having a cosmological constant Λ (Tinker et al. 2008; Boylan-Kolchin 2011) with its hypothetical weakly interacting particles – WIMPs (Merritt and Bertone 2005), warm dark matter (Stasielak 2006; de Vega and Sanchez 2011) whose particles would be sterile neutrinos (Boyarsky et al. 2009; Abazajian et al. 2012), which complicates the situation, and hot dark matter with neutrinos as carriers.

In particular, it is emphasized (Kamada et al. 2013) that the validity of the ΛCDM model on the galactic and the subgalactic scales has long been caught up in debate and that some researches argue that the number of dark matter subhalos is 10−100 times larger than the number of satellites observed around the Milky Way; so they argue that missing massive satellite problem can be solved only in the framework of warm dark matter in which carriers of the missing mass are sterile neutrinos with an energy about 2 keV. Quite recently de Vega et al. (2013) have considered the possibility of searching for sterile neutrino signatures in two experiments that are running at present, MARE and KATRIN, focused on the Rhenium and Tritium beta decays respectively. Hence they anticipate that sterile neutrinos will interact with a nucleus (or some nuclei) in the detector.

On the other hand, other researchers (Zolotov et al. 2012; Brooks et al. 2013) in support of the ΛCDM model and using super computers could show that the inclusion of stars that go supernova can alter the dark matter structure of galaxies driving dark matter out of the centers of satellites and this is the mechanism of lowering of the masses of the bright satellite galaxies; this brings the predicted and observed masses of the Milky Way's satellites into agreement.

The motivation for searching for WIMP is that cosmological observations require dark matter that is composed of a new kind of unknown particles. The weak force for their interaction requires new states as well. It is believed that WIMPs are naturally produced as thermal relics of the Big Bang with the densities required for dark matter; this WIMP miracle drives most dark matter searches (Feng and Kumar 2008). Referring to Ya. Zeldovich and his followers Feng and Kumar (2008), they point out that a particle's thermal relic density is

$$\Omega_X \propto 1/\langle \sigma \upsilon \rangle \sim m_X^2 / g_X^4 ,$$

where $\langle \sigma \upsilon \rangle$ is its thermally-averaged annihilation cross section, m_X and g_X are the characteristic mass scale and coupling entering this cross section, and the last step follows from dimensional analysis; m_X is associated with the dark matter particle's mass; the relic density is typically within an order of magnitude of the observed value, $\Omega_X \approx 0.24$. Their further analysis discloses a wide possible range for the mass: 10 MeV $\leq m_X \leq$ 10 TeV.

Since WIMPs do not experience electromagnetic interactions, they have to pass right through solid matter, for example a detector. The cross-section of their interaction with an atomic nucleus is considered close to that of the weak force, less than 10^{-40} cm^2. This means

that WIMPs may very rarely hit an atomic nucleus; nevertheless, such signature could be measured experimentally. Rocha et al. (2013) note that SIDM models with the cross-section per mass ratio ~ 0.1 cm^2/g consistent with all observational constraints.

However, so far no real success has been reached in the detection of WIMPs, which are so important for the ΛCDM model. In most cases the experiments searching for these hypothetical dark matter particles have become unsuccessful, though some others seem promising for further research. Some of these experiments are: the XENON dark matter search (Aprile et al. 2011), the Cryogenic Dark Matter Search (CDMS) detector (CDMS Collaboration, 2011), the DAMA/LIBRA detector (Bernabei et al. 2010; 2012), and others.

McCulloch (2012) suggested a model that modifies inertial mass, such that it correlates the gravitational interaction between objects correctly describing the Tully-Fisher relation, i.e. the anomalous behavior of the velocity of stars different from Kepler's law. Some researchers try to introduce new elements into the description of gravitating objects, such that dark matter is excluded automatically. For example, the physical vacuum might be considered as a fluid of virtual gravitational dipoles and the phenomenon of dark matter might be explained by the gravitational polarization of the quantum vacuum by the known baryonic matter (Hajdukovic 2011). On the other hand, by another hypothesis, strict conformal symmetry (local Weyl scaling covariance $g_{\mu\nu}(x) \to g_{\mu\nu}(x)\Omega^2(x)$, for a scalar field $\Phi(x) \to \Phi(x)\Omega^{-1}(x)$), might be postulated for all elementary massless fields, retaining standard fermion and gauge boson theory though with a modification of Einstein–Hilbert general relativity, the Friedmann equations and the Higgs scalar field model, with no new physical fields (Nesbet 2013). Conformal gravity and a conformal Higgs model remove trace elements, which are the major elements in the general relativity formalism, and such an approach allows one to fit empirical data on galactic rotational velocities, galactic halos, and Hubble expansion including dark energy without invoking dark matter.

The conceptual level just partly started by those last mentioned works.

Understanding the structure and nature of space are highly important, because they must be the foundation for the basic theoretical concepts of modern physics. Dark energy and dark matter introduce a dissonance in modern physics, which means that something is wrong with the fundamentals.

Dark energy is a constant energy density uniformly filling the space of the universe (i.e., postulated as a non-zero vacuum energy and pressure). The essence of dark energy is a subject of dispute. It reacts insignificantly with ordinary matter with the exception of gravity, has low density and a very homogeneous distribution.

In the USA the Dark Energy Task Force (DETF) was established by the Astronomy and Astrophysics Advisory Committee (AAAC) on future dark energy research. The DETF notes: "Dark energy appears to be the dominant component of the physical Universe, yet there is no persuasive theoretical explanation for its existence or magnitude. The acceleration of the Universe is, along with dark matter, the observed phenomenon that most directly demonstrates that our theories of fundamental particles and gravity are either incorrect or incomplete. Most experts believe that nothing short of a revolution in our understanding of fundamental physics will be required to achieve a full understanding of the cosmic acceleration. For these reasons, the nature of dark energy ranks among the very most compelling of all outstanding problems in physical science. These circumstances demand an ambitious observational program to determine the dark energy properties as well as possible" (Albrecht et al. 2006).

Kroupa (2012) writes about the dark matter crisis and falsification of the current standard model of cosmology; namely, he notes that the number and dark matter halo mass distribution of the Milky Way's satellite galaxies is in highly significant disagreement with the expectations from the standard model of cosmology. There is no physically known process

that may be able to solve the disagreements. He cites a long list of 22 complaints about the standard model of cosmology. Then he notes that the need to introduce dynamically relevant dark matter on galactic scales is required because the assumption that Einstein's field equations of 1916 be valid on galactic and cosmological scales led to a failure of them as soon as kinematical measurements in galaxies and of galaxies in galaxy clusters became available long after 1916. Kroupa (2012) points out that the speculation that exotic dark matter particles exist cannot be understood within the standard model of particle physics, as they have not been discovered by direct experiment despite a highly significant effort all around the world. Besides, he emphasizes that an effective gravitation appears to be non-Einsteinian and non-Newtonian, in particular, the true solution to gravitation may be Milgrom's suggestion that the effective gravitational force law at ultra-low accelerations $a_0 \approx 1.2 \times 10^{-10}$ m·s^{-1} (3.6 pc/Myr^2) (Milgrom 1983; 2009). No dark matter but rather modified gravity, modified Newtonian dynamics (MOND).

Incorporation of a MOND acceleration constant, which varies with redshift and an expansion history, and the introduction of neutrinos particles, allow one to describe experimentally observed galaxies that cannot be written by the usual Friedmann models (Angus and Diaferio 2011). Thus, no needs for peculiar dark matter particles behind the standard model of particle physics.

Kroupa et al. (2012) continuous to criticize the standard model of cosmology, which as they underline, is based on five postulates: 1) cosmological physics is based on assuming Einstein's field equation to hold on galactic and larger scales and for very small accelerations as are found in galactic systems; 2) all matter emerged in the Big Bang. The authors signify that these two postulates lead to an inhomogeneous and highly curved cosmological model, though the observed distribution of matter is rather homogeneous and flat; 3) an inflation is additionally postulated to drive the universe to near flatness and homogeneity briefly after the Big Bang; 4) the structures and their kinematics based on this postulate does not work correctly until cold or warm dark matter is hypothesized; 5) in addition, such model still in addition requires dark energy to driving the inflation.

Kroupa et al. (2012) conclude that cosmology requires a new paradigm. They focus on the extraordinary success of MOND in accounting for the observational data on galactic scales and its properties suggest that the expected underlying theory will contain a deep connection between the dynamics within local systems and the state of the universe at large.

Cosmic microwave background radiation discovered in 1964 (Penzias and Wilson 1964) is considered as the most important argument in support of the Big Bang model of the Universe. Since that the hot Big Bang model gradually gained popularity and pushed aside both the early Steady State models (Hoyle et al. 1993; 1994) and the ether theories (e.g., Thronhill 2001).

If the cosmic microwave background has the spectrum of a blackbody, then the universe might be treated as originated from a hotter, denser phase. Results on cosmic microwave background are considered to be of paramount importantance for cosmology. The NASA's COBE (COBE 2009) and WMAP satellites (WMAP 2011) and the Planck satellite of the European Space Agency (Rocha 2010) showed that the cosmic microwave background spectrum is that of a nearly perfect blackbody with a temperature of 2.725 K. The researchers claim this observation matches the predictions of the hot Big Bang theory.

However, these satellite results were strongly criticized (Robitaille 2007; 2009; 2010a; 2010b). Robitaille clearly points out that those experiments are fraud and the satellites' infrared antennas recorded signals of the Earth's oceans. He writes (Robitaille 2007): "the obscured resonances at ~4.63 ppm in the water spectrum would still have a signal to noise of ~5:1, if the water line had not contaminated this region... For WMAP, the signal to noise is less than 2:1, and the signal of interest is located at the same frequency of the

contamination… Signal suppression, by a factor of 100, or more, while still viewing the underlying signal, depends on the ability to control the source. This has been verified in numerous laboratories where the sample is known and where the correct answer can be readily ascertained. As such, it is impossible for the WMAP team to remove the galactic foreground given the dynamic range situation between the contaminant and the signal of interest… Relative to signal to noise, the WMAP team is unable to confirm that the anisotropic "signal" observed at any given point is not noise… The requirements for image stability in cosmology are well beyond the reach of both COBE and WMAP." "…with the aid of the Planck satellite, the electromagnetics laboratories of the world should be able to confirm or refute the existence of a ~3 K cosmic signal. The key to this puzzle rests in the understanding of the LFI (low frequency instrument) and reference targets... Enough evidence is already beginning to build … indicating that physics, astrophysics, and geophysics stand on the verge of a significant reformulation. In any event, the definitive proof that the monopole of microwave background belongs to the Earth has now been provided." (Robitaille, 2010b).

I often asked experimentalists at the conferences dealing with gravitational physics and cosmology: "Why do you think that the recorded signal, which you have discussed here, came from the sky but not from a neighboring room?" I have never heard an answer.

The criticism (Robitaille 2007; 2009; 2010a; 2010b) is quite serious and means that the existence of the cosmic microwave background radiation is very debatable. In any case such a radiation, if any, does not have a spectrum typical for the spectrum of a blackbody, which automatically eliminates the scenario of a hot beginning of the universe.

Are there any new ideas for the developing of cosmology? An interesting study carried out by Volovik (2003) in which he hypothesizes regarding the universe as a Helium droplet. Volovik's vacuum is similar to the ground state of quantum liquids; the "relevant ground state energy" that gravitates is $E_0 - \mu N$ not E_0; the universal equation of state for the vacuum of the universe (the same as for the quantum liquid): $\rho_{\text{vac}} = -P_{\text{vac}}$ and this equation exactly coincides with the equation of state of the cosmological constant in general relativity. This is mathematically equivalent to a zero-energy superfluid, although its fine morphology has gone unrecognized.

The constancy of the speed of light *c* is the pillar of special relativity. It is believed the constancy of the speed of light takes place in the four dimensional space-time whose space-time dimension number (four) is constant. However, switching of a possibility for the slicing of extra space dimensions, which provided by varying dimension numbers, gives rise to the emergence of a fine space structure. Varying dimension numbers are derived from varying speed of light theories (Barrow 2003; Magueijo 2003; Casado 2003; Ellis and Uzan 2003; Petit and d'Agostini 2007); the speed of light is treated as a parameter that varies in time. There are arguments demonstrating that the value of *c* is not a constant in vacuum (Santilli 2006). On the other hand, the possible variation of *c* in the context of the present accelerating universe is not permitted under the variable Λ models (Ghosh et al. 2012).

So we can see that dark matter, Big Bang, dark energy and cosmology as a whole are veiled with an impenetrable turbidity. On the other hand, a theory of dark matter recently proposed by the author (Krasnoholovets 2011) was based on a detailed mathematical theory of the ordinary physical space and the concept of subquantum physics developed in the strictly defined space with its peculiar structure, rules and properties. Below, referring to the physical meaning of cosmology, we consider the Einstein equations, features of metrics and how matter and the gravitational laws emerge in the space considered as a tessellated lattice of primary topological balls (section 2), then consider the Friedmann solutions and show how dark energy emerges in the universe constituted as the tessel-lattice (section 3), after that we demonstrate how in the tessel-lattice gravitational laws resolve the dark matter problem

(section 4). Then we exhibit our devices that measure flows of mass and provide the reader with our first experimental data of astrophysical measurements of massive signals (section 5).

2. Einstein field equations, metrics and the gravitation

2.1. General relativity

In the general theory of relativity the Einstein-Hilbert equations, or more exactly a set of 10 coupled nonlinear partial differential equations,

$$R_{\mu\nu} - \frac{R}{2} g_{\mu\nu} + \Lambda g_{\mu\nu} = \frac{8\pi G}{c^4} T_{\mu\nu} \tag{1}$$

connect the metric tensor $g_{\mu\nu}$ of the curled space-time with properties of matter that fills the space-time and is characterized by the stress-energy tensor $T_{\mu\nu}$. Here, $R_{\mu\nu}$ is the Ricci curvature tensor, R is the scalar curvature, Λ is the cosmological constant, G is Newton's gravitational constant, c the speed of light in vacuum. Components of the metric tensor $g_{\mu\nu}$ represent the gravitational potential in the chosen point of space-time.

Since both the Ricci tensor $R_{\mu\nu}$ and scalar curvature R depend on the metric in an intricate nonlinear way, Eq. (1) are really equations for the metric tensor $g_{\mu\nu}$. That is why researchers first of all try to investigate the metric tensor.

The classical example is the Schwarzschild metric (Schwarzschild 1916). The idea is to consider the square of a linear element of space-time ds^2 that does not change its form when turning spatial coordinates ξ^i around the axis that passes through the origin of coordinates. In the flat Minkowski space-time the square of the linear element in the spherical coordinates

$$ds^2 = -c^2 dt^2 + d\rho^2 + \rho^2 d\phi^2 + \rho^2 \sin^2 \phi d\theta^2 , \tag{2}$$

which is generalized in general relativity by using the expression

$$ds^2 = -A(r)c^2 dt^2 + B(r)dr^2 + r^2 d\phi^2 + r^2 \sin^2 \phi d\theta^2 . \tag{3}$$

The functions $A(r)$ and $B(r)$ include the gravitational field of the central mass M as the Newtonian potential $-GM/r$, which after a long chain of transformations and calculations of the Christoffel symbols $\Gamma^{\beta}_{\mu\nu}$ and the Ricci tensor $R_{\mu\nu}$ becomes finally (in the presentation of the Hilbert's metric)

$$ds^2 = -\left(1 - \frac{2GM}{c^2 r}\right) dt^2 + \left(1 - \frac{2GM}{c^2 r}\right)^{-1} dr^2 + r^2 d\phi^2 + r^2 \sin^2 \phi d\theta^2 . \tag{4}$$

The majority of modern researchers associate a coordinate singularity in the Schwarzschild metric (4) with the existence of so-called black holes in the universe, which ostensibly have been observed by astronomers. On the other hand, some other investigators of general relativity strongly oppose the existence of black holes showing that black holes are

not a consequence of the theory of general relativity (Crothers 2005, 2010, 2011, 2012; Loinger 2002, 2007; Rabounski 2008).

The Schwarzschild metric is not unique. There exist a number of different metrics that satisfy the conditions of invariance of the square of a linear element of space-time ds^2 at transformation of coordinates that does not change the form of the element. For example, one of them is the Nordström metric $ds^2 = e^{2\varphi}\eta_{\mu\nu}dx^\mu dx^\nu$ where $\varphi = -GM/(c^2 r)$ is the gravitational potential and $d\sigma^2 = \eta_{\mu\nu}dx^\mu dx^\nu$ is the line element for the Minkowski flat space-time. This metric is interesting, as it starts directly from Minkowski's. The exact solution looks as follows

$$ds^2 = \left[1 - GM/(c^2\rho)\right]\left[-dt^2 + d\rho^2 + \rho^2(d\theta^2 + \sin^2\theta d\phi^2)\right]. \qquad (5)$$

By using the transformation $r = \rho\cdot[1 - GM/(c^2\rho)]$, the metric changes into

$$ds^2 = [1 + GM/(c^2 r)]^{-2}(-dt^2 + dr^2) + r^2(d\theta^2 + \sin^2\theta d\phi^2). \qquad (6)$$

Considering a Nordström type metric, a Schwarzschild like metric, which uses exponential functions, can be presented in the form (Baretti Machín 2012)

$$ds^2 = \exp[-2GM/(c^2 r)]c^2dt^2 - \exp[2GM/(c^2 r)]dr^2 - r^2 d\theta^2 - r^2\sin^2\theta d\phi^2. \qquad (7)$$

The metric (7) is specified with the absence of a coordinate singularity and at the same time expanding exponential factors, since all planetary motion takes place in the region where $2GM/(c^2 r) << 1$, we arrive at the Schwarzschild metric (4).

The Schwarzschild-Hilbert metric has advantages over others (Kruskal, Szekeres, Gödel and so on), because it can correctly describe classic experiments, such as the movement of the perihelion of Mercury, the bending of a light ray by the sun, the red shift spectral lines in the presence of the gravitational field, and the radio signal delay (the Shapiro effect).

Nevertheless, owing to the obvious success of general relativity, the problem of understanding gravitation still remains. Once again, eqs. (1) describe a connection between the matter and the space curved by this matter, though the gravitational potentials are concentrated in the metric components.

The most fundamental problem is how general relativity can be reconciled with the laws of quantum physics to produce a complete and self-consistent theory of quantum gravity. It seems this challenge cannot be resolved in principle because of principal differences in approaches to physical laws by microscopic quantum physics and phenomenological general relativity. Besides, general relativity does not look like a true physical theory but rather like an abstract mathematical theory.

In the case of general relativity, which abandoned the classical ether concept and introduced an abstract vague vacuum, we can distinguish six problems, *conceptual difficulties*, which do not have resolutions in the framework of relativity formalism:

1) a massive object can influence space-time but cannot be derived from it, because the unknown and undetermined parameter mass *M* is entirely separated from the phenomenological notion of space-time;
2) the equation (1), which connects space-time and matter, includes a metric that should be chosen by hands, i.e. artificially (for example, expression (3));
3) the formalism of relativity is failing on a microscopic scale as it does not pay attention to the wave nature of matter; for instance, one can see this in a recent work (Salih et

al. 2012) in which the authors simply decrease the scale to microspace but do not touch the wave nature of the microscopic world. At distances equal compared to or less than the object's de Broglie wavelength the formalism of general relativity has to give way to an approach based on microscopic consideration;

4) general relativity is founded on the basic Newtonian term $-GM/r$, but cannot explain its origin;
5) general relativity does not offer any sort of particles/quasi-particles, which will be able to realize short-range action in the gravitational attraction of objects and hence it is a theory based on an action-at-a-distance phenomenological approach with the speed *c*, the same as the Newtonian theory (this one acts immediately, and also quantum mechanics whose long-range action also falls within the range of its conceptual difficulties); regarding the quasi-particles *gravitons* we can say that, based on the studies of other researchers (Loinger 2007) as well as experimental results (Krasnoholovets and Byckov 2000), these are abstract mathematical objects absent in real nature;
6) light, which plays an exceptionally important role in relativity, has to be massless in the theory; however, light carriers, photons, transfer momentum and energy and therefore by the principle of equivalence, photons must have non-zero mass;
7) it is complete unclear how to involve the formalism of general relativity in the study of the gravitational interaction of an ensemble of massive points in which pair potentials must be paramount important.

In addition to these critical items we should mention that the formalism of general relativity does not include dark matter and dark energy in its consideration.

2.2. Submicroscopic concept of gravity

2.2.1. Space structure, generation of matter and the quantum laws

The submicroscopic concept based on the constitution of physical space (Bounias and Krasnoholovets 2003; 2004) and submicroscopic mechanics (Krasnoholovets and Ivanovsky 1993; Krasnoholovets 1997, 2002), which allow a detailed theory of gravity to be derived introducing a radically new approach to the problem of gravitation and quantum gravity in particular.

The theory of physical space was build as a pure mathematical theory based on set theory, topology and fractal geometry (Bounias and Krasnoholovets 2003; 2004). The theory shows the necessity of the existence of a primary topological ball. Such balls completely fill space forming a tessellation lattice named the tessel-lattice. The tessel-lattice is provided with special rules. The size of a cell equals the Planck size $l_{\text{Planck}} = \sqrt{\hbar G / c^3} \approx 1.162 \times 10^{-35}$ m.

Classically, a measure is a comparison of the measured object with some unit taken as a standard. This signifies that one can introduce matter through a change in a cell of the tessel-lattice. Hence a local deformation of the degenerate tessel-lattice, which emerges at switching a fractal volumetric deformation of a cell, can be associated with the physical notion of mass. Such deformation can migrate from cell to cell or can scatter by cells. A stable symmetric volumetric deformation of a cell is associated with the creation of a massive particle. Thus mass is identified with a change of the volume of a fractal-deformed cell: The mass m_A of a particulate ball A is a function of the fractal-related decrease of the volume of the ball:

$$m_A \propto (V^{\text{deg. cell}} / V^{\text{part}} - 1) \cdot (\mathrm{e}_{\text{fract}} - 1)_{\mathrm{e}_{\text{fract}} > 1} \tag{8}$$

where $V^{\text{deg. cell}}$ is the typical average volume of a cell in the tessel-lattice in the degenerate state; V^{part} is the volume of the kernel cell of the particle; (e) is the Bouligand exponent, and $(e_{\text{fract}} - 1)$ the gain in dimensionality given by the fractal iteration. Just a volume decrease is not sufficient for providing a ball with mass, since a dimensional increase is a necessary condition (there should be a change in volumetric fractality of the ball).

Note that other researchers also point to a discrete space: "this is the effervescent Grid… Matter is not what it used to be. It consists of small, more-or-less stable patterns of disturbance in the Grid… Usually the metric field is taken to be fundamental, but in many ways it resembles a condensate, and that view of it may become important… What we ordinarily call matter consists of more-or-less stable patterns of excitation in the Grid, which is more fundamental. At least, that's how things look today" (Wilczek 2009).

So, the physical space is treated as a real substrate with its inner discrete structure, the tessel-lattice. The degenerate state of the tessel-lattice can be correlated with the physical notion emptiness. The tessel-lattice becomes the origin of matter; therefore, we may start from *the theorem of something* and determine major concepts fundamental physics operates with, instead of the usual *the theorem of everything* that tries to unify all fundamental interactions without understanding the basic figurants of these interactions.

The interaction of a moving particle-like deformation with the surrounding lattice involves a fractal decomposition process.

Submicroscopic mechanics of a particle moving in the tessel-lattice was developed in a series of works (Krasnoholovets and Ivanovsky 1993; Krasnoholovets 1997, 2002). Poincaré (1906) and de Broglie (1925) hinted to the principles of the motion, but the readers did not take their words into account. In particular, Poincaré noted that a particle, as a singularity of the ether, moves in it surrounded by the ether's excitations. De Broglie suggested that a point particle is guided by a real phase wave and he introduced two major relationships for a particle accompanied with such wave

$$E = h\nu, \qquad \lambda = h / p, \tag{9}$$

where ν and λ are the wave's frequency and wavelength, respectively, and E and p are the particle's energy and momentum. However, other physicists called such union of two different physical entities a 'wave-particle'.

In submicroscpic mechanics a particle moving in the tessel-lattice interacts with its cells, which results in the generation of excitations named *inertons* (because these excitations represent the particle's inertia). The Lagrangian of the submicroscopic mechanism includes three major parts: the kinetic energy of the particle, the kinetic energy of the ensemble of inertons and the energy of interaction of the particle and inertons. Schematically the Lagrangian can be shown in the form

$$L = \tfrac{1}{2} m\dot{x}^2 + \tfrac{1}{2} \mu\dot{\chi}^2 - \frac{\sqrt{m\mu}\,\dot{x}\chi}{T} \tag{10}$$

where m and x are the particle's mass and the position, respectively, and μ and χ are the mass and the position of the inerton cloud of the particle, respectively; T is the period of collisions between the particle and the cloud of inertons.

The Euler-Lagrange equations based on the Lagrangian (10) indicate periodicity in the behavior of the particle. The solution for the particle exhibits oscillates the particle velocity between the initial value υ and zero along each section λ of the particle path

$$\dot{x}(t) = \upsilon \cdot [1 - |\sin(\pi t / T)|], \tag{11}$$

$$x = \upsilon t + \frac{\lambda}{\pi}\{(-1)^{[t/T]}\cos(\pi t / T) - (1 + 2[t/T])\}. \tag{12}$$

The particle's spatial amplitude is $\lambda = \upsilon T$. The same for the cloud of inertons: $\Lambda = cT$, where c is the speed of light – the velocity with which inertons are emitted from the particle at its collisions with oncoming cells of the tessel-lattice.

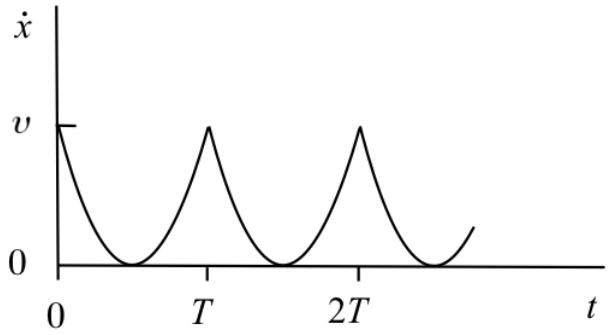

Figure 1. Velocity of a particle moving in the tessel-lattice versus time.

The solution for the inerton cloud of the particle shows that the cloud oscillates around the particle (Krasnoholovets 1997):

$$\dot{\chi} = (-1)^{[t/T]} c\cos(\pi t / T), \tag{13}$$

$$\chi = (\Lambda / \pi)\,|\sin(\pi t / T)| \tag{14}$$

The inerton cloud is emitted from the particle each odd section $\lambda / 2$ of the particle path and during the next even section $\lambda / 2$ these inertons return to the particle.

Amplitudes λ and Λ become connected by means of relationship

$$\Lambda = \lambda c / \upsilon. \tag{15}$$

The amplitude of spatial oscillations of the particle λ appears in quantum mechanics as the de Broglie wavelength. The amplitude of the particle's inerton cloud Λ becomes implicitly apparent through the availability of the wave ψ-function. Therefore, the physical meaning of the ψ-function becomes completely clear – it describes the range of space around the particle, which is perturbed by the particle's inertons. The cloud's inertons play the role of carriers of the field of inertia of the particle.

The connection of such mechanics developed in the real space to quantum mechanics constructed in an phase abstract space becomes clear when the same problem is treated in the Hamilton-Jacobi presentation. The corresponding expression for the shortened action S_1 of the particle appears in the form

$$\frac{\left(\partial S_1 / \partial x\right)^2}{2m} + \tfrac{1}{2} m \left(\frac{2\pi}{2T}\right)^2 x^2 = E \tag{16}$$

which is the shortened action of a typical harmonic oscillator with a cyclic time period equal to $2T$. Introduction of the action-angle variables leads to the increment of the particle action within the cyclic period $2T$

$$\Delta S_1 = \oint p dx = E \cdot 2T \,. \tag{17}$$

This expression can also be rewritten via the frequency $\nu = 1/(2T)$. Besides, $1/T$ is the frequency of collisions of the particle with its inerton cloud. Then using the relation $E = m\upsilon^2/2$ we get

$$\Delta S_1 = m\upsilon \cdot \upsilon T = p \cdot \lambda \,. \tag{18}$$

If we equal the increment of action ΔS_1 to the Planck's constant h, we immediately obtain from expressions (17) and (18) the de Broglie's relationships (9).

This means that h is the minimal action of the periodic motion of a particle when the particle is guided solely by the tessel-lattice and any influence on the side of external fields or direct contacts with other physical systems does not disturb the particle.

The availability of relationships (9) allows one to obtain the usual Schrödinger equation (de Broglie 1986)

$$-\frac{\hbar^2}{2m}\nabla^2\psi(r,t) + V(r)\psi(r,t) = E\psi(r,t) \,. \tag{19}$$

In conventional quantum mechanics an undetermined 'wave-particle' is further substituted by a package of superimposed monochromatic abstract waves. It is this approximation that gives rise to the inequality $\Delta k \Delta x > 1$ for changes of the position Δx and the wave number Δk of the wave package under consideration; multiplying this inequality by the Planck's constant h, we derive the Heisenberg's uncertainty $\Delta p \Delta x > h$ (see p. 52 in de Broglie 1986).

However, as we have just shown, such an interpretation in terms of 'wave-particle' is a very crude approximation to the real process of the motion, which realistically includes two subsystems – the particle itself and the inerton cloud that oscillates around the particle. This means that the origin of the quantum mechanical commutator

$$\hat{p}\hat{x} - \hat{x}\hat{p} = -i\hbar \tag{20}$$

is not in the uncertainties between Δk and Δx, but in the relationships (9) whose origin lies in the oscillating motion of the particle under consideration and its cloud of inertons in each section λ of the particle's path, which is characterized by the quantum of action $\hbar$.

Just to show that the uncertainty principle is not so fundamental, the reader may read the study of Nobel Price winner Hans Georg Dehmelt (Van Dyck et al. 1976, 1986); in collaboration with other researchers he could, with high precision measurements, gauge a number of parameters of an electron practically at rest. Besides, in recent high-resolution scanning tunneling microscopy experiments it has been revealed that the interpretation of the

density of electron charge as a statistical quantity leads to a conflict with the Heisenberg uncertainty principle (Hofer 2012); the uncertainty principle was violated by close to two orders of magnitude.

Submicroscopic mechanics was verified experimentally in many different physical systems. It was demonstrated that the Earth rotating from the west to east around its axis generates a flow of inertons, which we amplified in a simple resonator (Krasnoholovets and Byckov, 2000). Those amplified inerton waves influenced samples cut of razor blades, which were put in the resonator. The samples were studied by using an electron microscope. It was observed that the fine morphological structure of the edge of each razor blade indeed changed; a crude morphological structure remained the same. Hence the expected changes in the structure of the test specimens caused by the Earth's inerton field were in fact convincingly fixed in micrographs.

The submicroscopic concept started from the idea that electrons in atoms or in a metal should be treated as extended objects, but not point-like: an electron together with its inerton cloud has the length equal to their de Broglie's wavelength and the electron's inerton 'wings' spread up to the distance $\Lambda = \lambda c / \upsilon$ (15) in transversal directions around the particle, which for electrons in an atom and a metal is around 10 nm. Hence, the cross-section of the electron's inerton cloud is $\sim \Lambda^2 \approx 100$ nm^2. Thus, such an object is able to absorb *N* photons simultaneously, which can be considered an anomalous photoelectric effect (Krasnoholovets, 2001a). The corresponding probability was calculated and was applied to describe tens of different experiments on generation of photoelectrons in gases and a metal. The results are completely satisfactory. Indeed, if the intensity of a laser pulse is 10^{16} to 10^{18} W/cm^2, we can estimate a mean distance between photons in the flux of the laser pulse as 3-4 nm. Then the number of photons, which bombard the electron's inerton cloud is $\Lambda^2 / d^2 \approx 10$. In other words, the size of the electron (jointly with its inerton cloud) is large enough and can absorb up to 10 photons from a laser flux simultaneously. The total energy of these 10 photons exceeds the ionized potential of atoms in a gas (or the work function in a metal).

The freezing of fluctuating molecules in aqueous solutions affected by an inerton field was demonstrated experimentally (Krasnoholovets, Skliarenko and Strokach 2006; Andreev et al. 2007).

Binding of electrons into electron droplets became possible only due to an elastic attraction of electrons in the electron droplet (Krasnoholovets, Kukhtarev, Kukhtareva, 2006). Our rigorous experimental results manifested that the formation of stable electron clusters containing about 10^{10} electrons occurred due to the absorption of inerton radiation by photoelectrons where the inerton radiation originated from the crystal surface illuminated by a laser beam.

2.2.1. Generation of gravity

Submicroscopic mechanics considered above looks like a kinetic theory of a particle that collides with its inerton cloud.

The understanding of gravity starts from understanding the reasons why inertons emitted by a moving particle come back to it.

This is possible if inertons are not solid, but flexible quasi-particles. The same properties must be inherent in the case of the tessel-lattice. The interaction of a moving particle-like deformation with the surrounding lattice involves a fractal decomposition process. An inerton is generated at each collision of the particle with oncoming cells of the tessel-lattice: the particle loses a fragment of its mass, which is transferred into an emitted inerton. A number of inertons emitted by the particle passing the section $\lambda / 2$ until the stop, is of the order of

$\lambda / l_{\text{Planck}} \sim 10^{25}$ (if the particle's de Broglie wavelength $\lambda \sim 10^{-10}$ m). So inertons start having the velocity of light *c* and a mass m_{inert} that may vary from inerton to inerton (Krasnoholovets 2001b). At the distance of Λ from the particle an inerton stops having no mass but gaining a tension, which is demonstrated in Fig. 2. This is a typical oscillating process when a deformation changes to a tension and vice versa. Then at the distance Λ the tessel-lattice as a whole pushes the inerton back to the particle and the inerton hopping from cell to cell acquires its mass again and finally is absorbed by the particle transferring the mass m_{inert} on to it.

Note that the situation with the particle's inertons is similar to the situation with the particle itself. Within the section λ, due to the emission and re-absorption of the particle's inerton cloud, all parameters of the particle undergo periodical changes (Krasnoholovets 2010): velocity $\upsilon \to 0 \to \upsilon$; mass $m \to 0 \to m$ and the tension $0 \to \Xi \to 0$; electric charge $e \to 0 \to e$ and the magnetic charge, i.e. monopole state $0 \to g \to 0$; particle shape: beanlike $\to$ spherical $\to$ beanlike (such internal motion manifests itself in conventional quantum mechanics as a half-integer spin, i.e. snin-1/2).

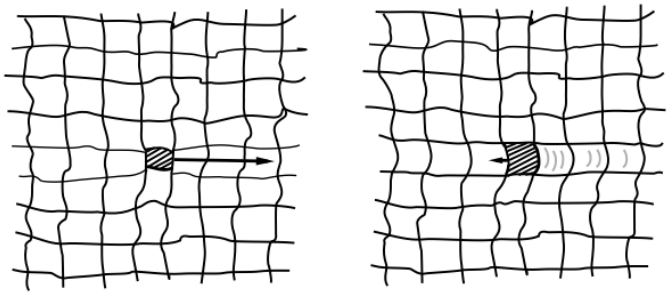

Figure 2. Inerton from the particle's inerton cloud: *a* – the inerton in the vicinity of the particle where it possesses a mass m_{inert} (the deformed cell); *b* – the inerton at the largest distance from the particle. Here, the inerton acquires a tension, or rugosity ξ_{inert} (the tense cell). This tension strains the tessel-lattice that due to the elasticity reflects the inerton back to the particle.

So since inertons transfer fragments of the particle's mass, they become not only carriers of inert properties of the particle but also play the role of carriers of gravitational properties of the particle. First of all we should describe how inertons irradiated by the particle come back to it returning fragments of its mass as well as the velocity. The behavior of the particle's inertons can be studied in the framework of the Lagrangian (Krasnoholovets 2008)

$$L = -m_0 c^2 \left\{ \frac{T^2}{2m_0^2} \dot{m}^2 + \frac{T^2}{2\Lambda^2} \dot{\vec{\xi}}^2 - \frac{T}{m_0} \dot{m} \nabla \vec{\xi} \right\}^{\frac{1}{2}}. \qquad (21)$$

Here, *T* is the time period of collisions of the particle and its inerton cloud; $m(\vec{r}, t)$ is the current mass of the {particle-inerton cloud} system; $\vec{\xi}(\vec{r}, t)$ is the variable that describes a local distortion of the tessel-lattice, which can be called a tension (or rugosity). In other words, we introduce a new variable $\vec{\xi}$ for the particle, which means that the mass is not an

absolute value but variable. A variation in mass should occur in case of a moving particle (de Broglie 1967). A similar behavior occurs in the case of a moving electric charge, when it periodically is transferred to the magnetic monopole state in each section of the particle's de Broglie's wavelength (Krasnoholovets 2003).

The Euler-Lagrange equations for variables m and $\vec{\xi}$ are

$$\frac{\partial^2 m}{\partial t^2} - \frac{m_0}{T}\nabla\dot{\vec{\xi}} = 0, \tag{22}$$

$$\frac{\partial^2 \vec{\xi}}{\partial t^2} - \frac{\Lambda^2}{m_0 T}\nabla\dot{m} = 0. \tag{23}$$

For the system, which features the radial symmetry, variables m and $\vec{\xi}$ are functions of only the distance r from the particle and the proper time t of the {particle + inerton cloud}-system. In this case we preserve only radial components in both variables, which enables us to rewrite equations (22) and (23) in the spherical coordinates as follows

$$\partial^2 m/\partial t^2 - (c^2/r)\partial^2(rm)/\partial r^2 = 0, \tag{24}$$

$$\partial^2 \xi/\partial t^2 - (\Lambda^2/m_0 T)(\partial/\partial r)\partial m/\partial t = 0 \tag{25}$$

where the Laplace operator Δ is presented in the spherical coordinates as $\Delta m = \frac{1}{r}\frac{\partial^2}{\partial r^2}(rm)$.

Thus the availability of the radial symmetry and the simple boundary and initial conditions (Krasnoholovets 2008) allow the solutions to equations (24) and (25) in the form of standing spherical waves, which exhibit the dependence $1/r$,

$$m(r,t) = C_1 \frac{m_0}{r}\cos\frac{\pi r}{2\Lambda}\left|\cos\frac{\pi t}{2T}\right|, \tag{26}$$

$$\xi(r,t) = C_2 \frac{\xi_{\max}}{r}\sin\frac{\pi r}{2\Lambda}(-1)^{[t/T]}\sin\frac{\pi t}{2T}. \tag{27}$$

These solutions exhibit the dependence $1/r$, which is typical for standing spherical waves.

The solution for the distribution of mass (26) shows that at a distance $r << \Lambda$ the time averaged distribution of mass of inertons along the radial ray, which originates from the particle, becomes

$$m \approx l_{\text{Planck}}\frac{m_0}{r} \tag{28}$$

In this region the tension of space, as followed from the solution (27), is $\xi \approx 0$.

In such a manner in the space around the particulate cell a peculiar relief is formed, a deformation potential $\propto 1/r$ that spreads up to a distance of $r = \Lambda$. In this range cells of the tessel-lattice are in the contraction state and it is this state of space, which is responsible for the phenomenon of the gravitational attraction. In fact from the distribution (28) we may easily obtain the Newton's gravitational potential

$$u = -G\frac{m_0}{r} \tag{29}$$

where the Newtonian constant of gravitation G plays the role of a dimensional constant.

We may anticipate that a similar pattern should take place around a massive object whose gravity is induced by all its entities. Indeed, entities vibrate in the neighborhood of their equilibrium positions. This occurs in the solid, liquid and gas phases, although in the latter two phases oscillations of entities near equilibrium positions are not stable, and in the gas phase resemble thermal chaotic motion. In any case amplitudes of these oscillations are nothing but the entities' de Broglie wavelengths.

It should be emphasized that the behavior of the speed of an oscillating entity is exactly the same as shown in Fig. 1 for the case of a rectilinearly moving particle. Hence vibrating entities of the massive object oscillating in the tessel-lattice produce inerton clouds, which of course overlap. Due to the overlapping a total inerton cloud of the object is formed. The spectrum of inertons is similar to the spectrum of vibrating entities. For instance, if we have a solid sphere with a radius R_{sph}, which consists of N_{sph} atoms, the spectrum of acoustic waves consists of $N_{\text{sph}}/2$ waves with the wavelengths $\lambda_n = 2an$ where a is the lattice constant (i.e. mid-distance between nearest atoms) and $n = 1, 2, 3, ..., N_{\text{sph}}/2$. Note if the lattice constant in a solid is equal to circa 4×10^{-10} m, the lattice constant for protons in the Sun has the same order, about 1.5×10^{-10} m.

At the same time inertons, which accompany acoustically vibrating atoms, produce also their own spectrum and the wavelengths of these collective inertonic vibrations can be estimated by expression

$$\Lambda_n = 2anc/\upsilon_{\text{sound}}, \tag{30}$$

which is the consequence of the relationship (15).

Also note that the behavior of these collective inerton oscillations obeys the law of standing spherical waves, i.e. the dependence of the front of the inerton wave must be proportional to the inverse distance from the source irradiating the wave, $1/r$. For instance, a solid sphere with volume 1 cm^3 includes around 10^{22} atoms; putting the velocity of sound $\upsilon_{\text{sound}} \approx 10^3$ m/s and the distance between atoms 0.5 nm, we obtain for the amplitude of the longest inerton wave: $\Lambda_{N/2} \sim 10^{18}$ m. Therefore up to this distance the inerton field of the solid sphere is able to propagate in the form of the standing spherical inerton wave. We may now apply the same consideration to the solid sphere studied, which has been done above for the gravity of a particle. In particular, expressions (26) and (29) is also applicable for the case of a massive object; at distance $r << \Lambda_{N/2}$, which for the solid sphere of volume 1 cm^3 is still a cosmic distance. It is interesting that light takes about 2 years to cover the distance $\Lambda_{N/2} \sim 10^{18}$ m. Note in the case of a material ball with the radius 10 m, its standing inerton waves reach the boundary of the universe, which is estimated by the radius of about $\mathbf{10^{26}}$ m.

At the same time, as has recently been found by the author (Krasnoholovets 2013a), that short wavelength vibrations of atoms in a solid are responsible for the so-called Casimir effect. In this effect associated with the edge of the Brillouin zone, the gravitational potential depends on the distance as $1/r^3$ and short inertonic waves spread only to a distance of r equal to $\Lambda_1 = 2ac/\upsilon_{\text{sound}} \leq 1$ μm.

Thus we are able to derive Newton's gravitational potential (29) also for a macroscopic object in terms of short-range action provided by inertons, carriers of mass entities of objects. If averaged in time, a mass field around the object studied can be considered as a stationary

gravitational potential.

Now let us consider the gravitational interaction between two objects, taking Poincaré (1906) note into account that an expression for the gravitation should include the velocity of the attractive object. Recently this has been accented again, i.e. that the law of gravitation has to take into account of the relative speeds of moving masses (Guy 2010).

The sub-microscopic approach (Krasnoholovets 2009) points to the fact that the gravitational interaction between objects must consist of two terms: (i) the radial inerton interaction between masses *M* and *m*, which results in the classical Newton gravitational force

$$F_{\text{Newton}} = G\frac{Mm}{r^2}\ , \tag{31}$$

and (ii) the tangential inerton interaction between the central attracting mass *M* and the rotating attractable mass *m*, which is specified by the tangential component of the motion of the test mass *m*.

Indeed, components of the inerton cloud's velocity in the vicinity of the particle, which moves with the velocity $\vec{\upsilon}$, are: $\vec{\upsilon}$ along the particle path and $\vec{c}$ in the transversal directions (Fig. 3). The same should be valid for a moving macroscopic object, because individual inerton clouds of vibrating entities in the object overlap forming a total inerton cloud. In the total inerton cloud inertons migrate by the same rule as is the case for inertons of a separate particle: move far away of the object and then return back to it.

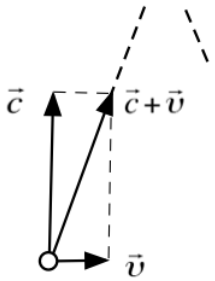

Figure 3. Components the particle's inerton velocity: $\vec{\upsilon}$ is along the particle path, $\vec{c}$ is in the direction transversal to the particle path.

Let a satellite with a mass *m* enveloped in its total inerton cloud rotate around the attracting mass *M*. The inerton cloud of the orbital mass *m* touches the central mass *M* is partly absorbed by it, which results in the reciprocal interaction between masses *M* and *m.* Components of the velocity of this total inerton cloud are $\vec{c}$ along the radial line and $\vec{\upsilon}_\perp$ in the tangential direction (Fig. 4). Hence the total inerton velocity in the satellite's inerton cloud is

$$\hat{c} = \sqrt{c^2 + \upsilon_\perp^2} \tag{32}$$

Then the kinetic energy of these inertons is $mc^2 \cdot (1 + \upsilon_\perp^2 / c^2)$.

If the speed of inertons is only c, than the square of a liner element should be written in line with the Minkowski metric,

$$ds^2 = c^2 dt^2 - d\vec{r}^{\,2}. \tag{33}$$

However, since the speed $\hat{c}$ (32) is present in the motion of the particle's inertons, which exceeds the speed of light, the square of a linear element should look as follows

$$ds'^2 = c^2 dt'^2 - d\vec{r}^{\,\prime 2}, \tag{34}$$

The time t is the proper time of the particle and t' is the proper time of the particle's inertons. Since these inertons travel faster than c, the relationship between these two times has to be as follows: $\sqrt{1+\upsilon_\perp^2/c^2}\,dt' = dt$. Then equating the linear elements ds^2 and ds'^2 to zero we derive an equation

$$dr'^2 = dr^2/(1+\upsilon_\perp^2/c^2). \tag{35}$$

Now we can solve the problem of how to introduce the tangential velocity into the Newton expression (31) for the radial attraction of two gravitating masses m and M (Fig. 4). The real trajectories of inertons of the orbital mass m do not go along the radial line r but have a small shift ahead following the velocity $\vec{c}+\vec{\upsilon}$ of inertons of the orbital mass m; in other words, their trajectory is going along the line r'. Integrating right and left hand sides of eq. (35) we get

$$r'^2 = r^2/(1+\upsilon_\perp^2/c^2). \tag{36}$$

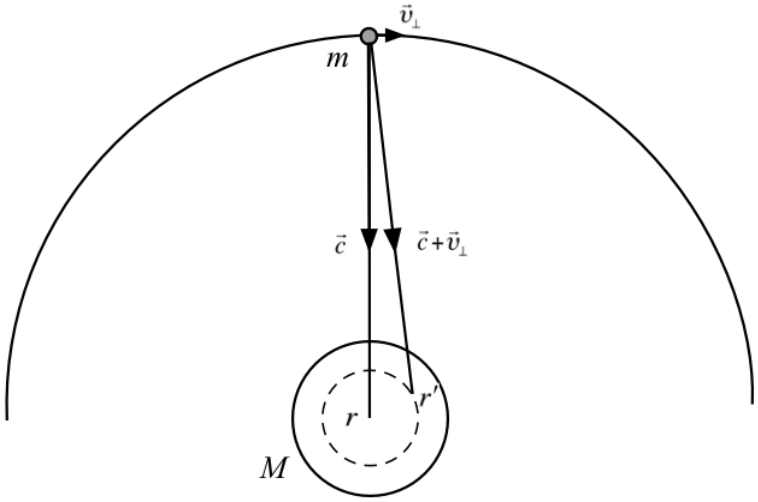

Figure 4. Orbital motion of the mass m around the central massive object with the mass M. Orthogonal components of the velocity of the inerton cloud of the orbital mass are equal to $\vec{c}$ and $\vec{\upsilon}_\perp$. Due to the tangential component $\vec{\upsilon}_\perp$ the line of attraction between the masses M and m shifts from the centre of the mass M and the effective radius r' of the attraction becomes shorter than r.

Substituting in expression (31) r^2 for r'^2 from expression (36) we obtain

$$F = G\frac{Mm}{r^2}(1+\upsilon_{\perp}^2/c^2)\,. \tag{37}$$

Then for the gravitational interaction of the orbital mass m with the central mass M we have

$$U = -G\frac{Mm}{r}\left(1+\frac{r^2\dot{\varphi}^2}{c^2}\right), \tag{38}$$

where we put for the tangential velocity $\upsilon_{\perp} = r\dot{\varphi}$.

Expression (38) was successfully used to obtain exactly the same equations and the solutions for such problems as the motion of Mercury's perihelion, the deflection of starlight by the Sun, and the gravitational redshift of spectral lines (Krasnoholovets 2009). Besides, this approach allowed the derivation of the Shapiro time delay effect (Krasnoholovets 2013b).

In contrast to orthodox quantum theory and general relativity, the submicroscopic concept allows us to derive the Newton gravitational potential (29) and introduce the corrected version of Newton's law of gravitation (38).

Our research has shown that the Schwarzschild-Hilbert metric (4), which represents properties of the geometry of space-time of a point mass M at rest, implicitly includes the second term of physical interaction associated with the orbital motion of a test mass m in the location of the latter (38).

Fractality of the tessel-lattice and fractality of balls, which compose the tessel-lattice, are responsible for the real geometry of physical space. This means that space-time of general relativity is disclosed as the four dimensional space of the tessel-lattice. In the tessel-lattice a convolution product represents the fundamental metrics of the ordinary physical space where the embedding part allows the description by the following relation (Bounias and Krasnoholovets 2003b)

$$\mathrm{D4} = \int\left(\int_{dV}(d\vec{x}\cdot d\vec{y}\cdot d\vec{z})\right) * d\Psi(w) \tag{39}$$

where dV is an element of space, and $d\Psi(w)$ a function accounting for the extension of coordinates to the 4th dimension through convolution ($*$) with the volume of space.

The fourth dimension reflects the space fractality, i.e. fractality of the tessel-lattice's balls. Time determined as a natural parameter through the path, can change only when balls, which form the path, shrink. Therefore non-linear components of metric of general relativity shall be considered as a mapping of original shrunk balls of the tessel-lattice (Krasnoholovets 2013b).

3. Cosmology and dark energy from the submicroscopic point of view

3.1. The modern paradigm and its problems

Cosmology is the science about the universe in general, the most general laws of the universe formation, structure and evolution. General laws of largest-scale structures and dynamics of the universe are studied by means of cosmological models. Modern cosmology is

based on Einstein's general relativity, especially the Friedmann model of the expansion of the universe (Friedmann 1922). The metric in the corresponding Einstein field equations is the Friedmann–Lemaître–Robertson–Walker metric (Friedmann 1922; Lemaître 1931; Robertson 1935; Walker 1937); it describes a homogeneous, isotropic expanding universe.

A very popular theme in cosmology is the beginning of the universe, which allegedly started from the Big Bang. The idea was formed soon after first works of Friedmann and Lemaître on the model of the expanding universe (Lemaître 1931).

In modern literature the Friedmann equations look as follows

$$\frac{\dot{a}^2 + kc^2}{a^2} = \frac{8\pi G\rho + \Lambda c^2}{3}, \tag{40}$$

$$\frac{\ddot{a}}{a} = -\frac{4\pi G}{3}\left(\rho + \frac{3P}{c^2}\right) + \frac{\Lambda c^2}{3}, \tag{41}$$

where the parameter k takes the values 0, 1, -1 and determines whether the shape of the universe if flat, a closed sphere or an open 3-hyperboloid; $a(t)$ is the scale factor; $H = \dot{a}/a$ is the Hubble parameter; Λ is the cosmological constant; ρ is the density of matter; P is the internal pressure. In cosmology an important parameter is the density parameter defined as

$$\Omega \equiv \frac{\rho}{\rho_c} = \frac{8\,\pi G\rho}{3H^2}, \tag{42}$$

where ρ_c is the critical density. The total density parameter is subdivided to a series of components:

$$\Omega = \Omega_{\mathrm{m}} + \Omega_{\mathrm{rel}} + \Omega_{\Lambda}, \tag{43}$$

where Ω_{m} is the mass density including baryonic mass and dark matter, Ω_{rel} is the effective mass density of relativistic particles (light and neutrinos), Ω_{Λ} is the effective mass density of the dark energy related to the cosmological constant Λ.

The standard model of cosmology focuses on measurement and determination of the cosmological parameters (Freedman 2000).

On the other hand, the Friedmann model and the related Big Bang theory meet severe difficulties. The first one is the problem of singularity. The solution leads to the conclusion that in the initial moment $t = 0$ the radius of the metagalaxy was zero and hence the density of matter in that moment equaled infinity. Such singularity contradicts the whole physical experience.

The second one is the problem of horizon. It is believed that the microwave background radiation comes from widely separated parts of the universe. However, these regions are so separated that they cannot even communicate by means of signals travelling with the speed of light. The question is: why do these regions have exactly the same temperature 2.7 K? If in the past the metagalaxy was divided into many causally non-related regions, then how can we resolve a problem associated with the observed amazing isotropy of the metagalaxy? How could different parts of the metagalaxy causally unrelated adjust to each other, so that by now a perfect isotropic (spherical or quasi-spherical) geometry has emerged? To resolve this paradox, the Big Bang theory simply assumes the needed level of uniformity…

The third is the flatness problem. The observations point out that the universe has very

low geometrical curvature in its space-time (it is nearly flat). So logically it is very unlikely that the universe indeed started from the Big Bang.

The forth is the monopole problem. Grand unified theories of physical interactions predict the existence of very massive particles called magnetic monopoles that should have been created at the Big Bang. However, these particles still have not been discovered. So, the problem is: where are the monopoles?

Moreover, some researchers formed a list of 30 problems associated with the Big Bang (The Top 30 Problems with the Big Bang, 2002)

Researchers try to solve these and smaller problems by introducing different novelties in the existing concepts. However, there is a possibility to remove these difficulties in a revolutionary way by changing the paradigm.

In fact, general relativity is a local theory written for an abstract massive point, which by the author's estimation cannot be less than the size 10 μm, because at a smaller size the laws of quantum physics start. At larger sizes the inner structure of matter has to influence the formalism of general relativity through vibrations of the matter's entities, which brings the matter's cloud of inertons into play.

The Fiedmann model looks very artificial itself: 1) a local theory was applied to the whole universe; 2) it is based on a non-physical metric (the so-called the Friedmann–Lemaître–Robertson–Walker metric). Friedmann (1922) was the first who introduced time into spatial components of the metric

$$ds^2 = R^2(x_4)(dx_1^2 + \sin^2 x_1 dx_2^2 + \sin^2 x_1 \sin^2 x_2 dx_3^2) + M^2(x_1, x_2, x_3, x_4)dx_4^2 \qquad (44)$$

where the coordinate x_4 is associated with the time t; $M^2(x_1, x_2, x_3, x_4)$ is a function (it is not a mass); $R(x_4)$ is proportional to the radius of curvature of space, so that the radius of curvature R can change over time. Today instead of Friedmann's designation $R(x_4)$ the curvature of space is written as $a(t)$ and called a scale factor. The Friedmann equations are derived from the Einstein-Hilbert equations (1) by using the metric (44).

However, in the Riemannian geometry, the scalar curvature (or the Ricci scalar) R is the simplest curvature invariant (scalar) of a Riemannian manifold. Its geometrical meaning is reduced to a single real number determined by the intrinsic geometry of the manifold near the point in which R is calculated. The scalar curvature R represents the difference in volumes of a geodesic ball written in a curved Riemannian manifold and the ball in Euclidean space. Thus R is a number, for example, 3.14. According to Friedmann, this number can depend on time t, namely, 3.14(t). Substituting in the metric (44) the scalar factor $R \equiv \text{const}$ with a factor depending of the time variable, $R(t) \equiv 3.14(t)$, one may try to solve the Einstein-Hilbert equations (1). However, how can such an approach be related to physics??

The cosmic microwave background, which is very important for the standard model of cosmology, seems a fiction (Robitaille 2007; 2009; 2010a; 2010b).

So, in physics there is no place for the Friedmann equations, the Big Bang and the cosmic microwave background. Then what are the origin of dark energy, the Hubble constant and other cosmological parameters? To understand the origin, researchers should go through an inner phase transition in their mind. Namely, they have to stop to consider themselves as ichthyologists who study the behavior of fish (i.e. stars and galaxies), but rather oceanographers who study the ocean as the whole (the universe that is a peculiar substrate in which stars and galaxies are excitations that behave like fish in the ocean).

3.2. The universe as a huge cluster in the tessel-lattice

The cellular structure of superclusters of galaxies and a sphere-like structure in aggregations of galaxies of smaller sizes are two problems of astrophysics. Any theory that attempts to explain the origin of large-scale structure of the universe must address these two problems.

Studies of relative scales in the empty-set lattice showed that the antifounded properties of the empty set provide existence of a lattice involving a tessellation of the corresponding abstract space with empty balls, i.e. the tessel-lattice (Bounias and Krasnoholovets 2003a, 2003b). Properties of a space at micro-scale are provided by properties of the spaces whose members are empty set units. In the mentioned works it was shown that particular levels of a measure of these units, quantum levels at relative scales, can be discerned.

A finite set of rational numbers inferring from a Cartesian product of a finite beginning section of integer numbers establishes a discrete scale of relative sizes. One possibility of a scaling progression covering integer subdivisions (n) consists in dividing a fundamental segment (n = l) by 2, then each subsegment by 3, etc. Hence the size of structures is a function of iterations (n). At each step (v_j) the ratio of the size in the dimension D is $(\prod v_j)^D$, so that the maximum ratio becomes

$$\Re \propto \left\{ \left(\prod v_j \right)^D \left(\prod v_j - 1 \right) \right\}_{j=1 \to n} . \qquad (45)$$

The manifold $(\prod v_j)^D$ is a commutative Bourbaki-multipliable indexed on the integer section $I = [1, n]$.

Expression (45) is of interested to us, as it allows one to establish a range and intermediate levels of the scale of size of objects composing a universe (Bounias and Krasnoholovets 2003b). Set theory and fractal geometry predict orders of size, different levels of organization (how many structural units this or that scale level requires in the universe). Predictable orders starting from the Planck scale, roughly comply with quark-like size (10^{10} to 10^{11} units), particle to atoms (10^{11} to 10^{17} units), molecules (10^{21}), human size (10^{28}), stars and solar systems (10^{40} to 10^{42}), up to the estimated upper limit (10^{56}) that could be bounded by a scale at (10^{60} to 10^{61}).

There should be further levels of higher scale universes, kinds of continued clusters with the following numbers of units: from 10^{82} to 10^{120}, then 10^{139} and 10^{142} to 10^{171}.

In the microworld, an introduction of an empty hyperset $\varnothing$ allowed us the implementation of almost countless number of iterations in a separate cell of the tessel-lattice. As we just showed above, the tessel-lattice allows different levels of self-organizations at high scales. In particular, it predicts the existence of galaxies, their unification and also the formation of a set of universes as well. The world of universes might look as depicted in Fig. 5.

Although the total space is subdivided into clusters and universes, the tessel-lattice should remain uninterrupted. This can be obtained through the different states of lattice balls inside universes and between them. Inside a universe they must be more contracted than outside the universe, which should support the tessel-lattice in a balanced state. In Fig. 6 such balls are shown for these two regions. A pair of charged particles emerges from a couple of balls in a universe. Leptons are strongly fractally deformed and quarks are maximally inflated. The charge state is determined by a polarization of the surface of a particulate ball (Krasnoholovets 2003).

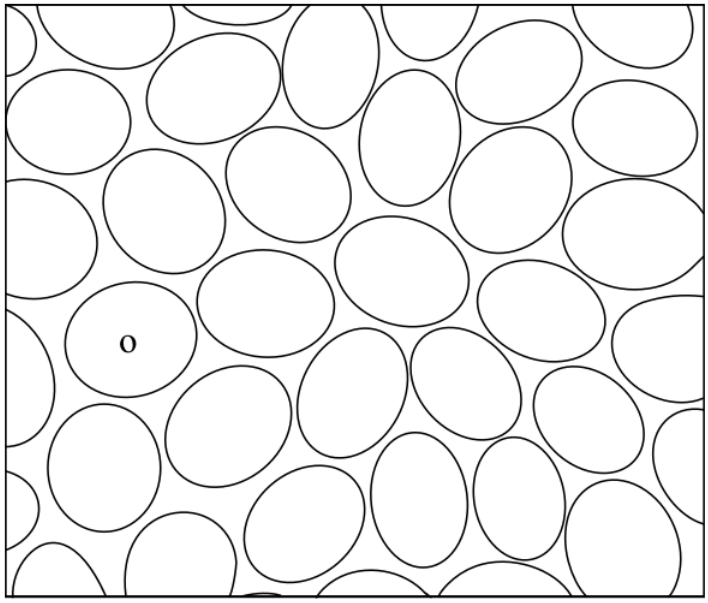

Figure 5. Manifold of spheroidal universes. The universe marked with the letter “O” would be ours. This is the pattern of one of the levels of higher scale universes, for examples, it can be the biggest cluster structure in the total world tessel-lattice.

What kind of organization, or ordering do topological balls experience in a spheroidal universe? To determine this, we may compare the problem with a macroscopic ball formed by a fluidic matter that shares also properties of gaseous and solid phases. Since the universe possesses a spherical shape, it should be characterized by the Laplace pressure $\gamma_{\text{univ}} \cdot (1/R_{\text{univ1}} - 1/R_{\text{univ2}})$ that forms a shell around the body of the universe. Hence the total pressure inside of the universe can vary from the center to the periphery. Namely, the size of a ball in the tessel-lattice may gradually increase from the center to the periphery (Bounias and Krasnoholovets 2003c); the radius of a ball in the *n*th coat can be approximated as follows:

$$\ell_n = \ell_0 + (n-1)b \tag{46}$$

where ℓ_0 is the minimal size of the ball at the center of the universe and b is a tiny increment of ℓ_0. In the continuous approximation the ratio ℓ_n / ℓ_0 (46) can be rewritten as $1 + x$ where $x = r / R_{\text{univ}}$; here, r is the radial distance from the center of the universe and R_{univ} is the radius of the universe.

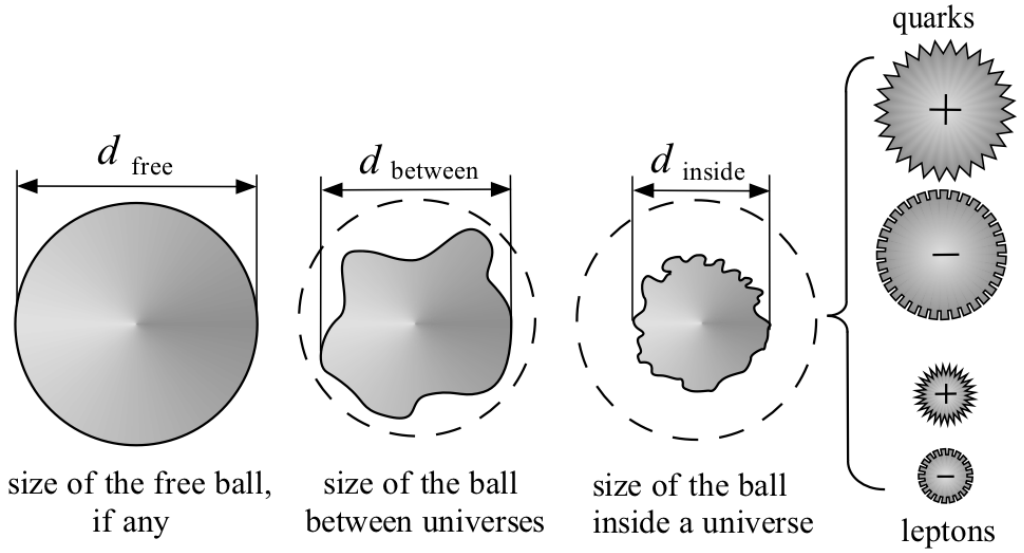

Figure 6. Topological ball, a primary subtle particle. Due to fractal deformations the ball shrinks, which is most significant insides a universe than in the interior regions.

Since we admit the variation of the ball size, we have to permit a variation in the pressure of the universe too, because the surface of balls changes towards the periphery of the universe. Since we allow the linear rule (43) for increasing the radius of a ball, the pressure at a point, which is removed at a distance r from the center of the universe, can be written as

$$P(x) = P_0 /(1+x)^2 \tag{47}$$

where P_0 is the pressure in the center of the universe; $x = r / R_{\text{univ}}$ is the dimensionless variable in which R_{univ} is the radius of the universe estimated by astronomers as equal to around 10^{26} m.

The mass of a ball inside the universe is defined as the ratio of its fractal volume to the middle volume of a ball from the region between universes (compare with expression (8)); such a “zero”-mass is the reference point for real masses (baryons) in the universe. The solution (26) for the distribution of mass around the massive object hints to a distribution of the density of topological balls inside the universe. This distribution should be a stable stationary solution for the cluster of a larger scale in the tessel-lattice, which is the universe. So, the distribution of the density of the tessel-lattice in the universe can have the form of a standing spherical wave

$$\rho(x) = \rho_0 \frac{\cos x}{1+x}, \tag{48}$$

where ρ_0 is the density of the tessel-lattice in the central part of the spherical universe. It is obvious that x has to vary from l_{Planck} to $\pi R_{\text{univ}} / 2$, such that at the boundary of the universe $\rho_{\text{bound. univ}} = 0$.

Formulas (47) and (48) show that remote distances can be overestimated by a measure

using a local gauge.

Expressions (47) and (48) allow us to calculate the finite sound velocity in the universe as the function of a distance x from its centre. In fact,

$$\frac{\partial P}{\partial \rho} = c^2, \tag{49}$$

where the derivative should be taken at the constant entropy, which is natural for the tessel-lattice. The equation (49) can be rewritten as follows

$$\frac{\partial P}{\partial x} \cdot \frac{1}{\dfrac{\partial \rho}{\partial x}} = c^2, \tag{50}$$

which results in

$$c(x) = \sqrt{\frac{P_0}{\rho_0}} \left. \frac{1}{\sqrt{(1+x)^2 \sin x + (1+x)\cos x}} \right|_{x \ll 1} \cong \frac{\sqrt{P_0 / \rho_0}}{1 + x + x^2}, \tag{51}$$

or finally putting $c \equiv \sqrt{P_0 / \rho_0}$ (the speed of light in the central part of the universe) and retaining only linear members by $x \equiv r / R_{\text{univ}}$ we get instead of expression (51)

$$c(r) \cong c \cdot \frac{1}{1 + r / R_{\text{univ}}} \tag{52}$$

It should be noted that in the tessel-lattice two kinds of basic deformations of a cell exist: a fractal volumetric deformation, which is associated with the physical notion of mass, and a surface fractal deformation, which is associated with the physical notion of electric charge (Krasnoholovets 2003). That is why two sound velocities exist in the tessel-lattice: fast longitudinal c_{inerton} and slower transversal c_{photon}. The general formulas should be the same, (51) and (52), in which, however, the density has a different nature – volumetric (mass) and surface (charge). In other words, for each ball there should be $\rho_{0\,\text{volume}}$ (responsible for mass-tension transitions) and $\rho_{0\,\text{surface}}$ (responsible for charge-monopole transitions). What is more, the inequality $\rho_{0\,\text{volume}} << \rho_{0\,\text{surface}}$ should hold, because, as is known from condensed matter physics, the longitudinal velocity exceeds the transversal one, which for our case means that photons are slower than free inertons, $c_{\text{photon}} << c_{\text{inerton}}$.

Below we will discuss expression (52) implying that it is recorded for photons, i.e., c is the speed of light in the center of the universe, and $c(r)$ is the speed of light at a distance r from the center towards the periphery.

Let us now consider Hubble's law, which is expressed by the equation $\upsilon = H_0 D$ where H_0 is the Hubble constant and D is a distance; υ is the recessional velocity, in km·s^{-1} (Hubble 1929). The parameters H_0 and D are not directly measured. They are found through a supernova brightness, which provides data on its distance, and the redshift $z = \Delta\lambda / \lambda$ of its spectrum of radiation (the fainter and smaller a galaxy appears, the higher is its redshift,

which typically is due to the Doppler effect). Hubble tied the brightness and redshift parameter *z* suggesting a surprising correlation

$$H_0 D = \frac{\lambda_{\text{measured}} - \lambda_{\text{source}}}{\lambda_{\text{source}}} c\,, \tag{53}$$

which suggests that more distant galaxies are moving faster away from us.

Thus by the relationship (53) the more distant galaxy is, the faster it is moving away from us, which means that the recessional velocity of a galaxy is proportional to its distance from us, $\upsilon = H_0 D$. The relationship (53) has been proved experimentally and is considered now as the major argument supporting the expansion of our universe.

However, let us rewrite the relationship (53) in forms

$$\lambda_{\text{source}} = \frac{\lambda_{\text{measured}}}{1 + H_0 D / c}\,, \qquad c / \nu_{\text{source}} = \frac{c / \nu_{\text{measured}}}{1 + H_0 D / c}\,. \tag{54}$$

From the second version of expressions (54) we can see that the other explanation of the phenomena of the recessional velocity is also possible. Namely, we may shift the change in the frequency, $\nu_{\text{source}} \to \nu_{\text{measured}}$, to the change in the speed of light: at a distance D from a terrestrial observatory the velocity of light can be different from the value of c measured in the central part of the universe. The appropriate relationship becomes

$$c(D) = c \cdot \frac{1}{1 + H_0 D / c}\,. \tag{55}$$

It is easy to see that the relationship (55) can be related to expression (52). In fact, let us check the equality $1/R_{\text{univ}} = H_0 / c$. Putting the Hubble constant $H_0 = 70$ km·s^{-1}·Mpc $= 2.265 \times 10^{-18}$ s^{-1} and the speed of light $c = 3 \times 10^8$ m·s^{-1}, we get for the radius of the universe $R_{\text{univ}} = 1.32 \times 10^{26}$ m, which is in agreement with the modern data. Hence the tessel-lattice model of cosmology naturally interprets the Hubble's law as a gradual decrease of the speed of light towards the periphery of the universe. No redshift, but instead the loss of speed of light owing to the step-by-step reduction of the density of the tessel-lattice in the framework of the universe. This also means that there is no dark energy in the universe, which allegedly accelerates galaxies after the hypothetical Big Bang.

The problem of the so-called accelerating expansion of the universe with high-redshift supernovae $z \approx 0.5$ (Perlmutter et al. 1998; Schmidt et al. 1998) has a natural elucidation in the framework of the present submicroscopic concept. The velocity of light is a function of the distance r from the center of the universe and the velocity $c(r)$ gradually decreases and especially dramatically drops near the boundary of the universe reaching the minimum value $0.39\,c$ at the boundary (see expression (51)). This means that the observed "accelerating expansion of the universe" can be accounted for by an abrupt dropping of the speed of photons in the vicinity of the boundary of the universe where the 42 Type Ia supernovae were detected. In fact, the derivative of the speed $c(r)$ (51) and (52) with respect to distance r is negative, which means a deceleration of photons at that point. However, if one does not take into account an abrupt reduction of the speed of light near the periphery, the supernovae could be perceived by an observer on the Earth to be accelerated in the direction from the center of the universe.

4. Dark matter

Dark matter is one more puzzle of modern physics, astrophysics and astronomy. The source of the problem relates to the perception of the universe as an empty reservoir filled with residuals of the Big Bang. However, the consideration of orderly physical space as the tessel-lattice removes all the difficulties in the description and comprehension of this phenomenon (Krasnoholovets 2011).

Stars are found in the tessel-lattice and their inner entities vibrate near their equilibrium positions. Due to the interaction with cells of the tessel-lattice the entities emit inertons, which form the total inerton cloud of the star inducing the Newton potential (29). This inerton cloud is distributed around the star as a standing inerton wave, which spreads up to the boundary of the universe. In an ensemble of stars a mutual overlapping of the stars' inerton clouds occurs. Standing inerton waves of the opposite sources should undergo an elastic interaction. For instance, a similar picture we can observe on the surface of water when water waves of two sources interfere, generating wavelets.

Therefore, standing inerton waves induce the gravitational potential (29) and, in addition, owing to the mutual scattering of counter propagating waves of nearest stars they introduce the elasticity in interstellar space.

The Hamiltonian of interacting stars can be written in a lattice model in the form

$$H(n) = \sum_s E_s n_s - \tfrac{1}{2}\sum_{s,s'} u_{ss'}^{\text{attract}}\, n_s n_{s'} + \tfrac{1}{2}\sum_{s,s'} u_{ss'}^{\text{repul}}\, n_s n_{s'}. \tag{56}$$

Here E_s is the additive part of the star energy (the kinetic energy) in the *s*th state. Then we have two kinds of pair potentials: the attraction and the repulsion components. So, in the Hamiltonian (56) the potential $u_{ss'}^{\text{attract}}$ represents the paired energy of attraction and the potential $u_{ss'}^{\text{repul}}$ is the paired energy of repulsion. All starts are considered as identical. The potentials take into account the effective paired interaction between stars located in states s and s'. The filling numbers n_s can get only two values in the model lattice: 1 (the *s*th knot is occupied) or 0 (the *s*th knot is not occupied). The signs before positive functions $u_{ss'}^{\text{attract}}$ and $u_{ss'}^{\text{repul}}$ in the Hamiltonian (56) directly specify proper signs of attraction (minus) and repulsion (plus).

The statistical sum of the system of interacting stars

$$Z = \sum_{\{n\}} \exp\bigl(-H(n)/k_{\text{B}}\Theta\bigr) \tag{57}$$

can be rewritten via the action S, which depends on three functions,

$$Z = \text{Re}\,\frac{1}{2\pi i}\int D\phi \int D\psi \oint dz\, \exp\bigl[S(\phi,\, \psi,\, z)\bigr]. \tag{58}$$

The complicated function $S(\phi,\, \psi,\, z)$ was evaluated for extremum (Krasnoholovets and Lev 2003). The minimum of the action S is reached when all stars are distributed by clusters, especially if each cluster includes the same number of stars. In this case the action for a cluster of *N* stars (allowing they obey the Bose statistics) becomes

$$S \approx \tfrac{1}{2}\{a(N) - b(N)\} \cdot N^2 \tag{59}$$

where the functions *a* and *b* are defined as follows:

$$a(N) = 3 \int_1^{N^{1/3}} u^{\text{repul}}(gx) x^2 dx / (k_B \Theta), \tag{60}$$

$$b(N) = 3 \int_1^{N^{1/3}} u^{\text{attract}}(gx) x^2 dx / (k_B \Theta) \tag{61}$$

In the case of the Boltzmann statistics the action for a cluster of N stars has the form

$$S = 2\{N \cdot [a(N) - b(N)] + N \ln \xi_0\} \tag{62}$$

where ξ_0 is the fugacity.

Knowing the explicit form of the action (59) or (62), one can derive the equation for the number of particles combined in a cluster: $\partial S / \partial N = 0$, which in addition requires holding of the inequality $\partial^2 S / \partial N^2 |_{N = N_{\text{in cluster}}} > 0$.

The pair potentials that enter equations (59)-(62) look as follows

$$u^{\text{attract}}(gx) = \frac{Gm^2}{gx} + \frac{GMm}{R}, \tag{63}$$

$$u^{\text{elast. repul}}(gx) = \tfrac{1}{2} m\omega^2 (gx)^2 \tag{64}$$

where m is the mass of a star; g is the lattice constant, the distance between neighbor stars in the model lattice); x is the dimensionless distance defined through a relation $r = gx$; ω is the radial frequency of oscillations of the mass m near its equilibrium position. Besides, in expression (63) we add a mean field formed by the whole galaxy, where M is the total mass of the whole system of stars and R is the effective radius of the system.

It should be noted that a quadratic potential $V(r) = \gamma_0 c^2 r^2 / 2$ was already used in the conformal theory of gravity to fit the observed behavior of galactic rotation curves (Mannheim and O'Brien 2010, 2011). The origin of the potential generated through the effect of cosmology on individual galaxies through all parameters had a completely different meaning originating from an abstract metric of a theory of long-range action despite its quantization.

The solutions for clusters of stars can be obtained for all the dimensions: 3D, 2D and 1D (Krasnoholovets 2011). All three cases were observed: bulk galaxies (Clowe et al. 2004), disc galaxies (Famaey and McGaugh 2013) and rings/arcs (Fort and Mellier 1994; Jee et al. 2007), respectively.

The most interesting are solutions for disc galaxies and bulk galaxies. Starting from the action (59), we get for a disc galaxy the following solution

$$N = \frac{3}{2} \frac{GM}{Rg^2 \omega^2}. \tag{65}$$

which means that all the stars of the disc galaxy are distributed by a plane cluster with the appropriate number N of stars. We may choose some typical values of the mass, the radius and the distance between stars in the galaxy: $M = 10^8 M_\oplus$, $R = 10$ kpc, $g = 1$ pc. The frequency ω of oscillations of a star near its equilibrium position in the cluster can be estimated from the equality of the centripetal acceleration that attracts a star to the center of the galaxy and the holding force that acts between stars in the cluster:

$$GM / R^2 - \omega^2 g = 0 . \tag{66}$$

From eq. (66) we get

$$\omega = \left(\frac{GM}{R^2 g} \right)^{1/2} \approx 2.1 \times 10^{-14} \text{ [s}^{-1}\text{]}. \tag{67}$$

Let us now evaluate the acceleration that each star experiences in the plane cluster:

$$a = GM / R^2 \approx 1.4 \times 10^{-11} \text{ m·s}^{-2}. \tag{68}$$

This value of the acceleration satisfies the conditions prescribed by Milgrom (Famaey and McGaugh 2012, 2013) $a << a_0 \cong 1.21 \times 10^{-10}$ m·s^{-2}. Thus we do not need to assume an incomprehensible modernization of Newton's law, i.e. the substitution of the force $\mathbf{F} = m\mathbf{a}$ by a significantly smaller force of undetermined nature $\mathbf{F} = m \cdot (\mathbf{a} - \Delta\mathbf{a})$ at $a << a_0$. Stars are distributed by clusters and each star is strongly bonded with the other $N - 1$ stars in the cluster. This bonding compensates the centripetal acceleration. Expression (66) demonstrates this balance of two competing forces. That is why a Keplerian law, $V \sim 1/\sqrt{r}$, is substituted for Milgrom's constant orbital velocity $V^4 = GMa_0$.

Let us now discuss the 3D cluster solution

$$N = \left(\frac{30}{11} \frac{GM}{Rg^2 \omega^2} \right)^{3/2} . \tag{69}$$

The parameters can be chosen as follows: the total mass $M \sim 10^{14} M_\oplus$, the radius $R \approx 250$ kpc and the central mass density $\rho_0 = 3.85 \times 6 M_\oplus$ kpc^{-3}. Putting for the mass of a star $m = M_\oplus$, we obtain the mean distance between stars: $g = (M_\oplus / \rho_0)^{1/3} = 4.25 \times 10^{16}$ m. Then the stability of the cluster in respect to its gravitational collapse is determined by the relationship (66): the gravitational attraction of stars to the centroid is retained by the elasticity of inerton waves in the cluster. The corresponding frequency of oscillating stars at their equilibrium positions owing to the overlapping of their inerton waves is

$$\omega = \left(\frac{GM}{R^2 g} \right)^{1/2} \approx 3.82 \times 10^{-13} \text{ [s}^{-1}\text{]}. \tag{70}$$

The acceleration to the centroid, which each star experiences in the spherical cluster, is

$$a = GM / R^2 \approx 2.24 \times 10^{-8} \text{ m·s}^{-2}. \quad (71)$$

The acceleration (71) is opposite to the inequality $a << a_0$ needed for the use of MOND. Besides, the acceleration (71) is not compensated by the acceleration caused by the elastic interaction in the cluster of N stars: $\omega^2 g \approx 6.2 \times 10^{-9}$ m·s^{-2}.

However, the origin of so-called dark matter is nothing but the same stars, which are involved in the mutual interaction through their inerton waves. Stars are floating in an elastic space. This elastic interaction is responsible also for a non-homogeneous distribution of stars, i.e. they assemble in clusters. Hence in a galaxy there must exist a non-equilibrium density distribution of mass. It is this regularity that has to be responsible for the correct rotation curve (Feng and Gallo 2008, 2011). By introducing a complicated distribution of mass in a disc galaxy Feng and Gallo (2008, 2011) managed to obtain the correct rotational curve profile even without an introduction of dark matter. But where is the origin for a no-homogeneous distribution of mass? The answer is obvious: the elastic interaction affects the density distribution and influences on the rotational curve profile bringing it to a law $\upsilon^4 = GMa_0$.

Basic concepts of gravitational lensing should also be modified – perhaps a point mass approach with a correction based on MOND or another model will require a substitution by an approach resting on the involvement of elastically interacting masses. In particular, it seems the deflection angle $\varphi = 4Gm/(c^2 r)$ of a point mass m, which includes the absolute value of the gravitational potential Gm/r, can be modified as follows

$$\tilde{\varphi} = \frac{4}{c^2}\left(\frac{Gm}{r} + \tfrac{1}{2}\omega^2 r^2\right); \quad (72)$$

In a cluster the second term in expression (72) tends to align the space deformed by the first term. This has to be typical for 2D clusters (i.e. clusters in disc galaxies). In the case of 3D clusters (rich clusters in galaxies) the second term may even prevail the first one, namely, the second term prolongs the deflection angle φ for larger distances at which the first Newton's term becomes already negligible.

The center of a galaxy that can be described as a cluster of stars possesses a peculiar property. This is a small region in which inerton standing waves of different stars interfere. Inerton waves deliver mass to this place, but the waves do not spread further and therefore the mass m is not transferred to the tension ξ as equations (22) and (23) prescribe. This region looks as an endpoint of standing inerton waves of each star of the galaxy. This is a kind of singular point, which might be observed by astronomers and interpreted as a black hole. Nevertheless, inertons do not disappear at this point but establish a special stationary relief of mass from stars to the endpoint supported by the equilibrium of the centripetal acceleration (generated by the rotating stars) and the centrifugal one (emerged as the linear response to the inerton wave pressure on the side of the elastic tessel-lattice).

The long-standing problem about the additional enigmatic acceleration of artificial satellites in the solar system has been debated for years. In particular, researchers discussed some Doppler shift anomalies for the Pioneers 10 and 11, Galileo, NEAR, Cassini, Stardust, Rosetta, Hayabusa, and MESSENGER, as well as the flyby anomalies (Lämmerzahl et al. 2008).

Based on data for the Pioneers 10 and 11 orbit determination and more detailed studies of all the systematics, a total error budget, i.e. an acceleration pulling the satellite Pioneer 10 to

the sun was determined as $a_{\text{Pioneer}} = 8.74 \times 10^{-10}$ m·s^{-2} (Anderson et al. 2002). However, later on the same researchers changed their opinion (Turyshev et al. 2012): they mention that since the spacecraft was facing the Sun, the solar energy was absorbed primarily by the high-gain antenna that largely shadowed the rest of the spacecraft from direct solar irradiation; the absorbed energy increased the high-gain antenna temperature and was then emitted as infrared radiation. A contribution on the side of this thermic radiation emanating from the antenna was estimated of the same value as the Doppler's shift.

However, the hypothesis of the thermal origin of the Pioneer 10 anomaly (Turyshev et al. 2012) has a significant flaw, because the further the distance of the satellite from the Sun, the lower is its heating by the Sun and hence the effect of the thermic radiation of the antenna should also be weaker. Unfortunately, the authors of the hypothesis did not pay any attention to this fact.

Lämmerzahl et al. (2008) also discussed other anomalies, such as the increase of the astronomical unit (the distance between the Earth and the Sun), the quadrupole and octupole anomaly, and dark energy and dark matter.

It seems likely that all the anomalies mentioned above are directly associated with the inerton elasticity of space, which is generated at the gravitational interaction of cosmic objects. In fact, a spacecraft moves through a viscous network formed by standing inerton waves of interacting stars, planets and other cosmic objects. Of course the viscosity of space has to slow the movement of satellites (through the switching of terms $\kappa\dot{r}$, $\frac{1}{2}\gamma r^2$, and the Navier-Stokes equation), which so far has never been taken into account by the staffs that led the spacecrafts. In particular, expressions (68) and (71) allow for the introduction of the viscosity of space in our galaxy related to the Milky Way's "dark matter".

In recent work (Turyshev et al. 2012) a realization of astronomical relativistic reference frames in the Solar System and its application to the GRAIL mission are presented. The authors develop the relevant relativistic coordinate transformations that are needed to describe the motion of the GRAIL spacecraft and to compute all observable quantities. This is made in a general relativistic model (calculations involve an expansion of the metric tensor and the Newtonian potential preserving a few terms in the expansion) with accuracy to 1 μm. They derive phase differences measured at both spacecraft, $n_{\text{AB}}(t\text{B})$ and $n_{\text{BA}}(t\text{A})$, together with the instantaneous delays measured at the points of signal reception at both spacecraft, $T_{\text{AB}}(t\text{B})$ and $T_{\text{BA}}(t\text{A})$. It can be argued beforehand that the data received from the satellites will have inaccuracies due to the neglect of the viscosity of space in which the satellite is moving.

5. First steps of inerton astronomy

Non-stability of cosmological physical factors that affected different biophysical, chemical physical and physical processes in a laboratory was studied by Sholl with collaborators (Shnoll et al. 2000, Shnoll et al. 2005; Shnoll 2001, 2009). For example, processing of six-year measurement data of alpha-activity of ^{239}Pu with the total of about 60,000 measurements showed regularity of patterns of histograms (the number of recorded counts per minute), namely, the highest probability of similarity nearest neighbors (the effect of near-field) and a clear circadian periodicity of similar histograms. They also observed a change in timing of histograms constructed by measurements of α-activity of ^{239}Pu on a ship in the Indian Ocean and in the laboratory near Moscow in 1988. A direct correlation with the position of the Moon in the sky (especially at the rising and setting of the Moon) and the form of histograms plotted by data of alpha decay of ^{239}Pu.

A coincidence of histograms was observed, which were recorded by measurements of γ-activity of ^{137}Cs at the Columbus Polarity Therapy Institute in Columbus by M. Sue Benford and J. Talnagi and α-activity of ^{239}Pu by S. Shnoll in Pushchino (Russia) during the period of 18-20 February 2001, separated by a distance of 12,000 km.

In the study of one-minute histograms (constructed for each of 60 one-second measurements of alpha activity of ^{210}Po) periodic signal repetitions were detected, "macroscopic fluctuations", which were associated rather with a sidereal day (1436 hours) but not the solar day (1440 hours). Many months of continuous studies pointed out to periodic cosmic fluctuations in the intensity of fundamental physical processes that manifested themselves each 546 hours (with a period of 22.75 days), 576 hours (with a period of 24 days), 648 (with a period of 27.0 days) and 672 hours (with period of 28 days).

Later on Shnoll and co-workers carried out experiments with collimators directed towards the Polar Star and the Sun, the West and the East, as well as with clockwise and counterclockwise rotations, then with GCP-generators, electronic noise generators, etc.

Shnoll (2009, 2012) concludes that factors determining shapes of modeled histograms may facilitate to reveal factors that determine the shapes of physical histograms; the physical processes, to which the changes of histogram shapes are due, in turn can be attributed to the motion of the Earth through cosmic space.

Fig. 7 depicts fluctuations of the decay constant of Tritium caused by non-stationarity cosmic factors of unkmown origin (recorded by our team), which is complete in agreement with observations of Shnoll (2009, 2012).

One more study of cosmic factors is related to the pioneering works of Kozyrev (Kozyrev 1977; Kozyrev and Nasonov 1978) who demonstrated the existence of a remote influence of a star, which affected the measuring transmitter (a resister), much early than the star became visible in the telescope. Those first results of 1970s then were confirmed by other researchers (Lavrentiev, Yeganova et al. 1990; Lavrentiev, Gusev et al. 1990) who noted that Kozyrev's and their observations of planets, stars and galaxies showed that in fact there exists a kind of an interaction, which modern physics does not consider. By their opinion the investigation of this kind of the interaction has an important meaning for the development of ideas of physics about the real constitution of space-time.

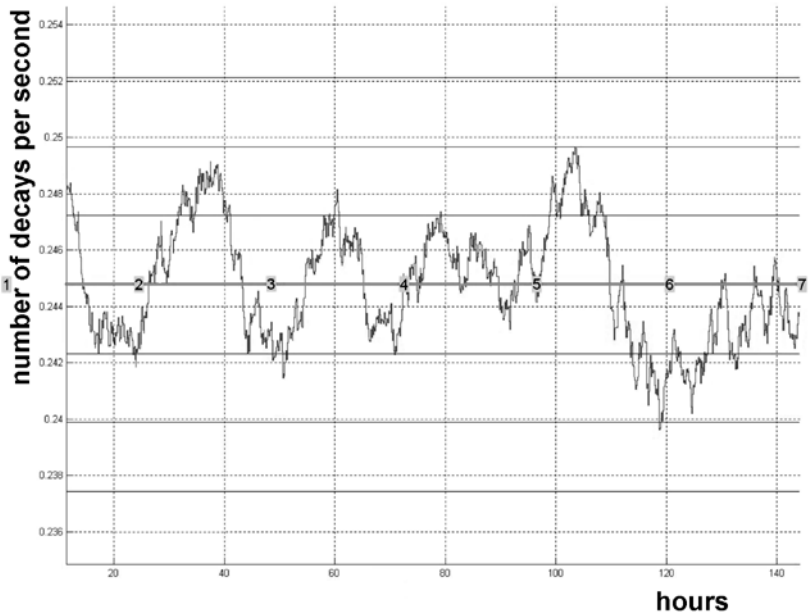

Figure 7. Fluctuations of the decay constant of Tritium recorded by our research team in 2010. The days of measurements are applied on the horizontal axis.

So, what was the reason for those Kozyrev's enigmatic superluminal rays? It seems plausible that they are related to free inertons irradiated by stars, i.e. inertons that escaping from the appropriate inerton clouds of stars and planets at fast non-adiabatic processes.

Free inertons liberated from inerton clouds of particles can migrate through space until other massive objects will absorb them. Since inertons are carriers of mass properties of matter, it will be interesting to launch astrophysical observations using appropriate inerton antennas, receivers, electronics and software. Inerton observatories will be able to yield pictures of the universe derived from inerton radiation (instead of the existing laboratories constructed for the detection of hypothetical gravitational waves, incomprehensible dark matter particles and other exotic particles).

Fig. 8 demonstrates the device 'Rudra' designed by our research team, which measures inertons. In the device two kinds of the antenna are used: a ferrite rod-type core and a disc-type piezoceramic. The measurement depends on the orientation of the antenna. The antenna absorbs a signal and the density of the antenna's material increases locally for a short time. Mechanical changes are transformed in the appropriate magnetic/electric polarization, which immediately influences the current of an electronic scheme. An amplifier increases the current to the level sufficient to launch the channel of signal recording. The frequency divider, interchanging switch and timer perform the adapting between the level of the signal and the discharge grid of the recorder. The device is designed on the principle of a counter: it counts arriving inertons that strike the antenna. When the antenna is put in a metal box that screens it of electromagnetic waves, the device continues to operate counting inerton signals. However, if a standard radio used for normal radio reception is placed in the same metal box, the receiver stops to function altogether.

Figure 8. The 'Rudra' inerton measuring device. The device is able to count inerton signals received by the antenna per second (i.e. can measure the intensity) and can also show the spectrum of absorbed inerton signals from a few Hertz to 100 kHz.

Fig. 9 demonstrates our recent device that can be called an inerton gravity-gradient meter. Its antenna consists of two quartz crystals functioning at the frequency of 10 MHz with an accuracy of 10^{-12}. Each of the crystals is set in its proper metal casing that completely screens the detector from the electromagnetic environment. A change in the orientation of one of the detectors immediately shows a disharmony between the resonance frequencies of 10 MHz. Since the device measures only inertons, this disharmony correlates with the density of an inerton pulse or inerton flow caught by the detector.

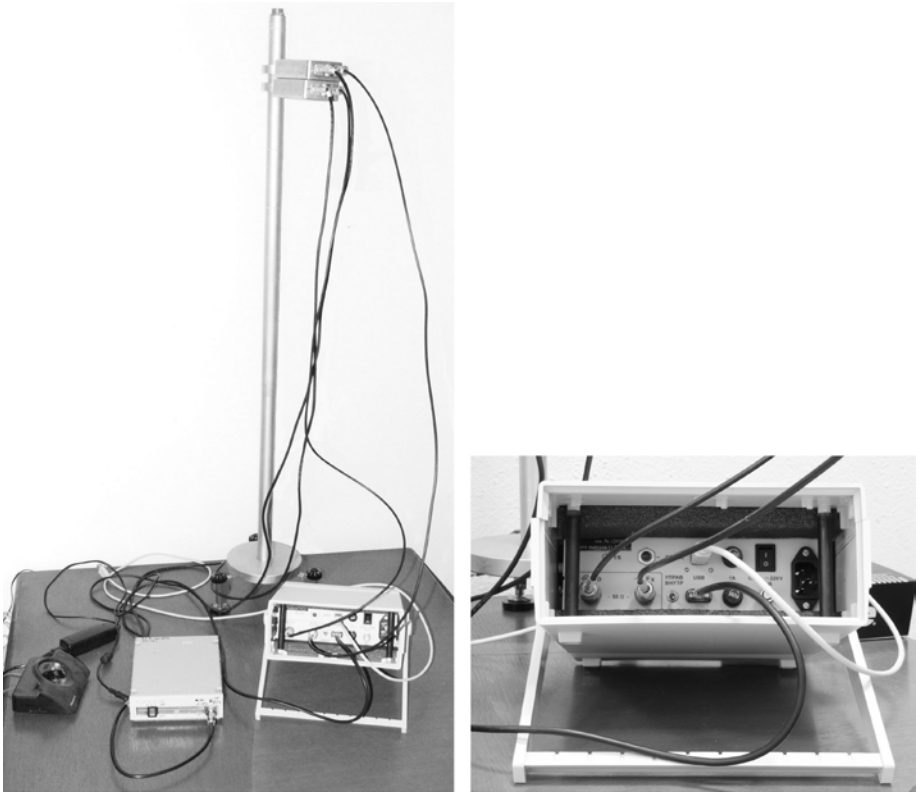

Figure 9. Inerton gravity-gradient meter.

Below, Figs 10-13, we present results of our measurements as a function of the antenna orientation and the time of measurement. The measurements were performed with a predecessor of the ‘Rudra’ device. The measurements were on purpose conducted at difficult conditions in a windowless room in a concrete building. Obvious measurements of the Earth’s inerton field exhibit the pronounced orientation effect: signals picked up along the West-East line are more intensive than signals received along the North-South line. A gradual decrease in the intensity of inertons along the West-East line and the increase of the intensity along the North-South line with time is associated with the proper rotation of the Earth when the antenna orientation with respect to the Sun gradually changes. In case of the West-East line of the antenna orientation the dip angle of inertons coming from the Sun begins to depart from normal, which means the decrease in absorption of inertons. In case of the North-South line of the antenna orientation, the dip angle of inertons coming from the Sun tends to the normal giving raise to an additional absorption of inertons.

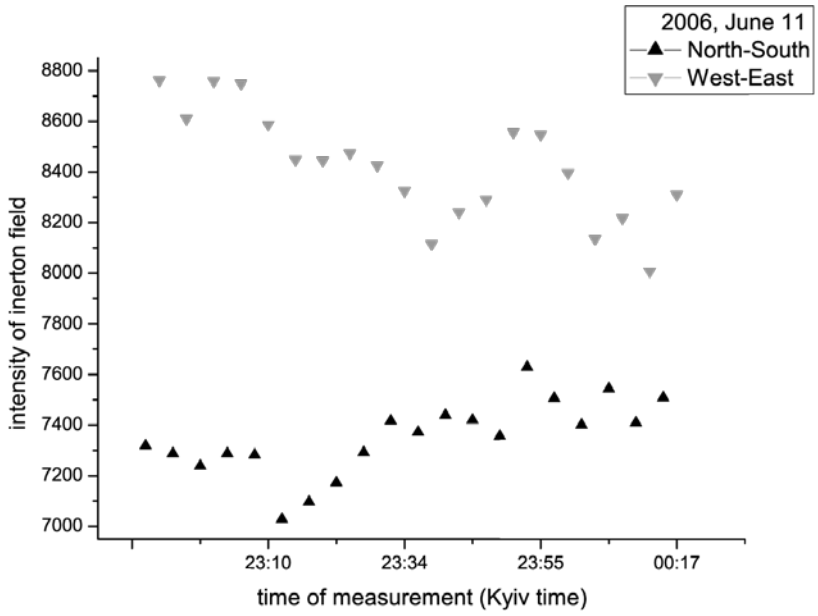

Figure 10. Intensity of inerton flow versus time of measurement. Quite warm night.

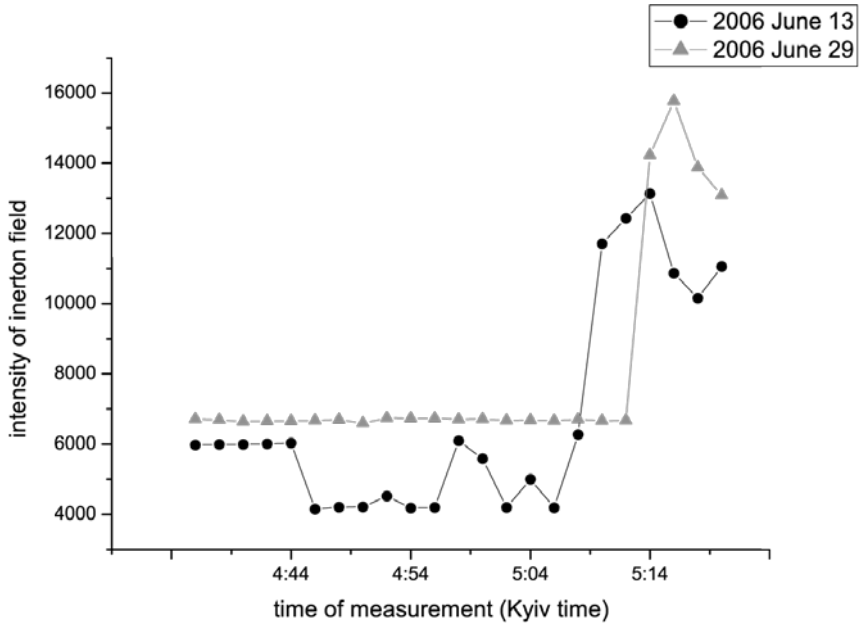

Figure 11. Intensity of the inerton field along the West-East line versus time. Nice and sunny days. Sharp splashes correspond to the time of sunrise.

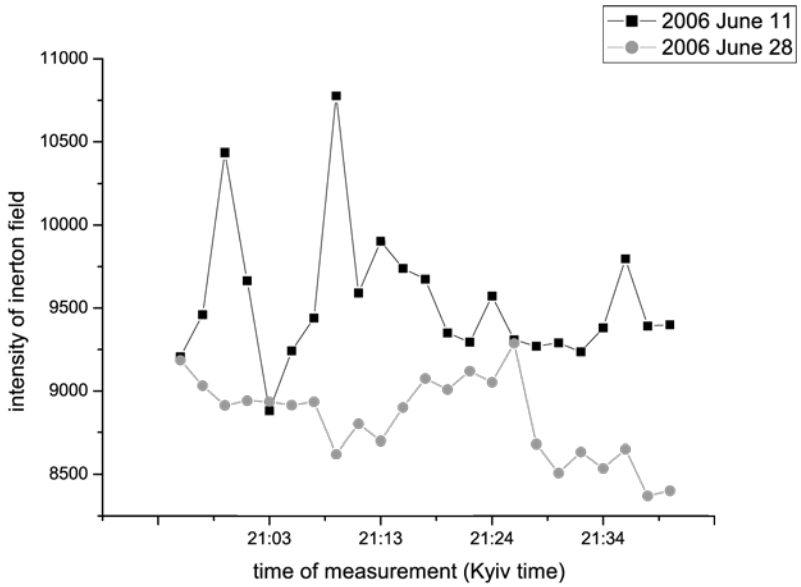

Figure 12. Intensity of inerton field at the moment of sunset versus time.

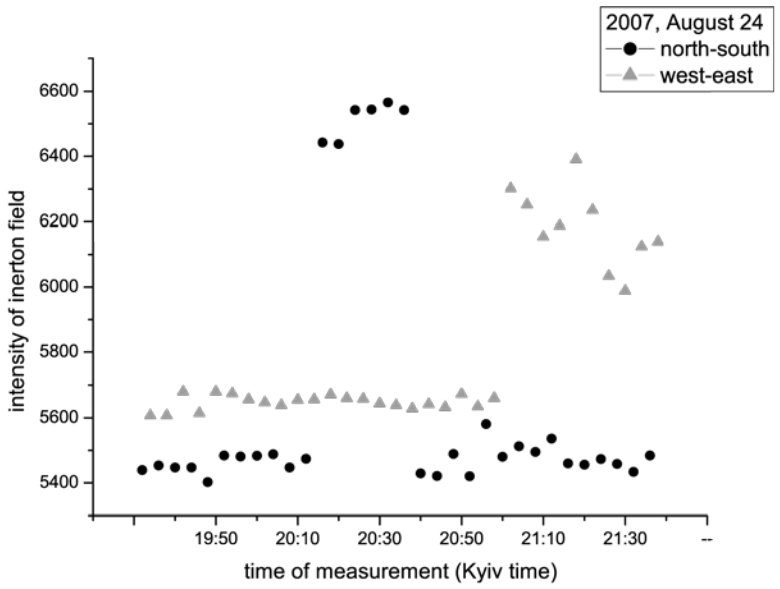

Figure 13. Intensity of inerton field at the moment of sunset versus time.

With the measurement of terrestrial inertons we can trace periodical modulations caused by the influence of solar inerton rays, Figs. 10 to 14. Fluctuations may be associated with the influence of solar inerton activity. Solar inertons introduce appropriate changes to the intensity of terrestrial inertons. These changes vary from 5 to 20 % probably owing to the rotation of the Earth. The most significant rise in inerton intensity is observed during the light period of the astronomical day. Meteorological factors also severely affect the measurements, which means that clouds saturated with water, the motion of clouds strengthened by wind and the rain are additional sources of inerton radiation on the surface of the Earth.

Figs. 14 and 15 exhibit the results of measurements obtained with our modern version of the 'Rudra' device (Fig. 8) at two mutually perpendicular positions of the antenna: the North-South line and the West-East line. The measurements were carried out in a cabin in a village south of Kyiv, Ukraine (latitude: 50 North, longitude: 30.5 East). There were no electromagnetic power sources in a radius of 25 km. The measurements were carried out on 26 November 2011.

Fig. 14 depicts data recorded early morning in the dark circa one hour before dawn. At the orientation of the antenna's surface along the West-East line the device recorded 82 ± 10 impulses per second with a ferrite antenna with a coil and 90 ± 10 impulses per second for the piezoceramic sensor. At the orientation of the two antennas along the North-South line, there were recorded 76 ± 10 and 69 ± 10 impulses per second, respectively.

One hour later (Fig. 15) in the dawn time we could see that the intensity of inertons significantly increased, as the energy of inerton impulses reached 5000 a.u. When the antennas were aligned along the West-East line the intensity of the inerton field increased by 400% (340 ± 30 impulses per second), while with the orientation along the North-South line it showed an increase 82% (92 ± 10 impulses per second).

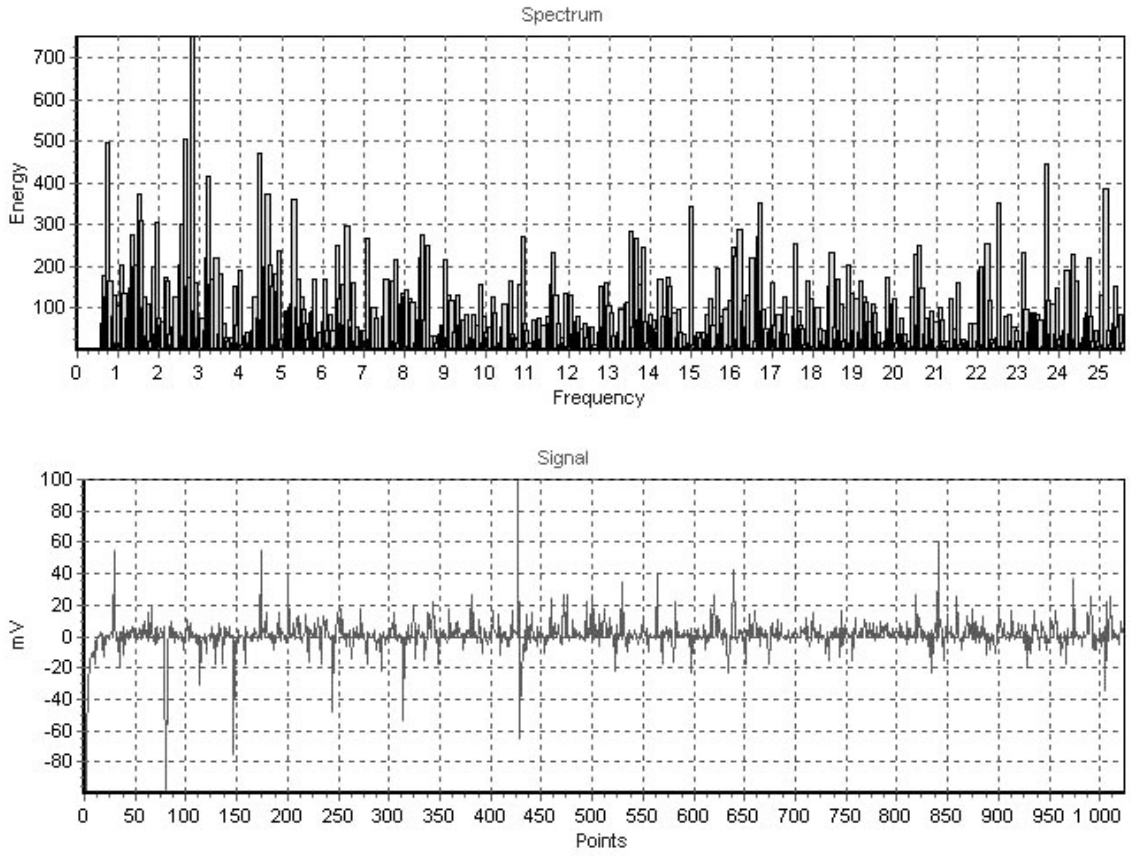

Figure 14. Record of inerton signals (bottom) and its frequency spectum decoding (in kHz, top) in the dark at 5:57 a.m. The antenna is the piezoceramic disc; the orientation "West-East".

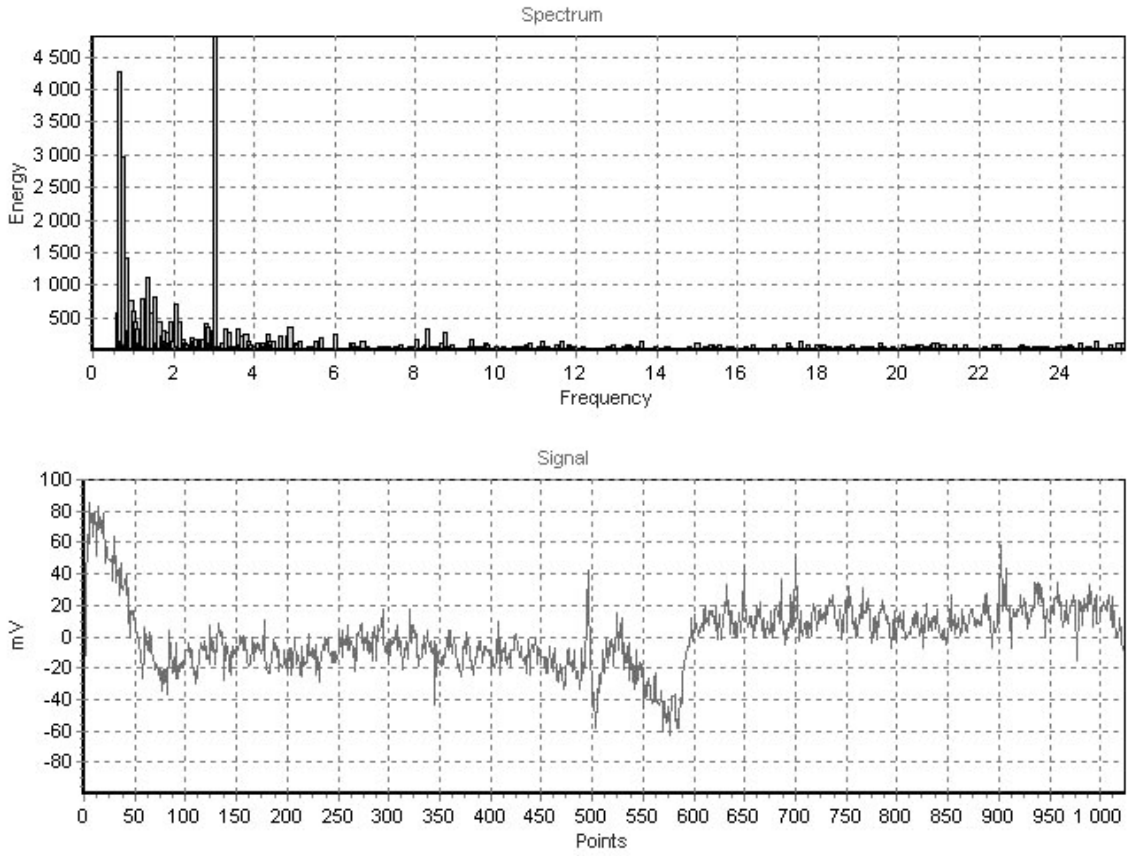

Figure 15. Record of inerton signals (bottom) and its frequency spectrum decoding (in kHz, top) during dawn at 6:56 a.m. The antenna is the ferrite rod with a coil; the orientation "West-East".

Basing on our measurements, we may conclude that the spectral decomposition of the recorded signals in the range of a few Hz to 100 kHz exhibits the densest inerton zone between 2 and 4 kHz. When the orientation of the antennas coincides with the West-East direction, the mentioned zone of frequencies is more clearly expressed than at the orientation of the antennas along the North-South line.

The 'Rudra' device can further be redesigned for astronomical observations. In particular, the behavior of inerton activity of the Sun looks extremely interesting and important; because the Sun is not only a globe of plasma and inner nuclear reactions, it is also the source of a huge dynamic mass, 1.99×10^{30} kg. This mass irradiates flows of inertons of different intensity and frequencies. We measured an influence of the solar inerton radiation on the Earth's background inerton field. We constantly observed changes in the Earth inerton filed associated with instability of atmospheric processes. For example, we recorded an unusual change in the spectrum associated with the Lunar eclipse that occurred in our place (Kyiv, Ukraine) on 15 June 2011.

Thus, inertons from outer space can be recorded at a laboratory on the Earth. We may study the intensity of inerton signals, the direction from which they arrive, their frequency, the degree of homogeneity of signals and we may also measure the velocity of inertons, which by preliminary estimation, is about two orders higher than the speed of light *c*. In our approach we are able to carry out a multidimensional analysis by using a one-dimensional channel (i.e. one procedure of measurement). Subsequently we can extract even very weak

signals (with signal to noise ratio of up to 1:1000 using special technology). We measure amplitude, frequency spectrum and time characteristics.

We are interested to collaborate with astronomers and astrophysicists in designing the first measuring system, an inerton observatory, which will be able to show amplitude, spectral and time characteristics of non-stationary signals in real time. The system will record inerton signals from the Earth atmosphere, from the Earth, the Sun as well as distant objects in the celestial sphere by means of different methods, namely:

- measurement of anomalies by using detectors on the basis of a piezoceramic disc or and/or a ferrite rod with a copper coil in a range of Hz up to hundreds of MHz;
- measurement using a high precision inerton gravity-gradient meter made on the basis of quartz crystals, developed and designed by our team (it can distinguish signals from background noise with a sensitivity of up to 10^{-12}); the vertical gravity gradient data can be gauged with an accuracy better than 0.1 Eötvös;
- measurement of cosmic anomalies by means of the point-by-point gauging of background radiation with a sensitivity of 10^{-10} using photomultipliers (radiation range from a few keV to many GeV);
- measurement using of Terra-hertz receivers.

In conditions of fixed or variable geometry we have to distinguish an anomaly that by its characteristics will be significantly weaker then the general background (i.e. we have to separate a very weak signal from the noise of the Earth, a star, nebula, etc.). We are able to do this with one-time measurement. The noise can be significantly higher than the signal that we will be searching for. The direction of the signal can also be undetermined, which requires special conditions: the necessity to have a position-sensitive component. Thus, the system will consist of a tracking facility and the four abovementioned measuring set-ups.

6. Conclusion

So far the universe has not been considered as a substrate that is governed by strict mathematical laws. The present work shows that real space can be described in the form of the tessel-lattice of primary elements, topological balls. Matter in the universe is a deformation of the tessel-lattice and hence any interaction between material objects involves space.

Dark energy is nothing but a peculiar distribution of topological balls in our universe considered as a huge-scale cluster in the total tessel-lattice.

The gravitational interaction, as a basic interaction in the universe, is derived directly from the behavior of the object studied in the tessel-lattice. The gravitational interaction between many objects induces in addition to the corrected Newton potential (38) also an elastic interaction. These two factors are responsible for the phenomenon known as dark matter, namely, a distribution of standing inerton waves around massive bodies creates an obstacle for travelling photons.

Until today the universe has been explored only in different spectra of photon radiation. Now a new possibility is presented – an examination of outer space through inerton rays, which are mass carriers of the gravitational interaction of cosmic objects. The investigation will require new kinds of astronomical equipment and appropriate inerton observatories, gateways to future inerton astronomy.

Acknowledgment

The author greatly thanks colleagues Yu. Zabulonov and V. Burtniak for the assistance in designing the devices for measuring inerton fields. Many thanks to A. Keder for critical reading of the manuscript.

References

Abazajian K. N., et al. (2012). Light sterile neutrinos: A white paper, arXiv:1204.5379 [hep-ph].

Albrecht A., Bernstein G., Cahn R., Freedman W. L., Hewitt J., Hu W., Huth J., Kamionkowski M., Kolb E. W., Knox L., Mather J. C., Staggs S. and Suntzeff N. B. (2006). Report of the dark energy task force, arXiv: astro-ph/0609591.

Anderson J. D., Laing P. A., Lau E. L., Liu A. S., Nieto M. M., and Turyshev S. G. (2002). Study of the anomalous acceleration of Pioneer 10 and 11, Phys. Rev. D 65, 082004 (55 p.); arXiv: gr-qc/0104064.

Andreev E., Dovbeshko G. and Krasnoholovets V. (2007). The study of influence of the Teslar technology on aqueous solution of some biomolecules, *Research Lett. Phys. Chem.*, Volume 2007, Article ID 94286, 5 pages; arXiv:1204.6062 [physics.gen-ph].

Angus G. W. and Diaferio A. (2011). The abundance of galaxy clusters in MOND: Cosmological simulations with massive neutrinos, *Mon. Not. R. Astron. Soc.* **417**, no. 2, 941-949; arXiv:1104.5040 [astro-ph.CO].

Aprile E., et al. (The XENON100 Collaboration) (2011). Implications on inelastic dark matter from 100 live days of XENON100 data. *Phys. Rev. D* **84** (061101).

Baretti Machín R. (2012). http://www.uprh.edu/rbaretti/Nordstrom3dic2012.htm.

Barrow J. D. (2003). Unusual features of varying speed of light cosmologies, *Phys. Lett.* **B564**, 1-7; arXiv: gr-qc/0211074.

Bernabei R., Belli P., Cappella F., et al. (2010). New results from DAMA/LIBRA, *Eur. Phys. J. C* 67, 39–49.

Bernabei R., Belli P., Cappella F., Caracciolo V., Cerulli R., Dai C. J., d'Angelo A., Di Marco A., He H. L., Incicchitti A., Ma X. H., Montecchia F., Sheng X. D., Wang R. G., Ye Z. P. (2012). No role for muons in the DAMA annual modulation results, *Eur. Phys. J. C* **72**, 2064.

Benítez-Llambay A., Navarro J. F., Abadi M. G., Gottlöber S., Yepes G., Hoffman Y., and Steinmetz M. (2013). Dwarf galaxies and the cosmic web, *Astr. J. Lett.* **763** (2), L41.

Bounias M. and Krasnoholovets V. (2003a). Scanning the structure of ill-known spaces: Part 1. Founding principles about mathematical constitution of space, *Kybernetes: The Int. J. Systems & Cybernetics* **32**, no. 7/8, 945-975, Eds.: L. Feng, B. P. Gibson and Yi Lin; also arXiv: physics/0211096.

Bounias M. and Krasnoholovets V. (2003b). Scanning the structure of ill-known spaces: Part 2. Principles of construction of physical space, *Kybernetes: The Int. J. Systems & Cybernetics* **32**, no. 7/8, 976-1004, Eds.: L. Feng, B. P. Gibson and Yi Lin; also arXiv:physics/0212004.

Bounias M. and Krasnoholovets V. (2003c). Scanning the structure of ill-known spaces: Part 3. Distribution of topological structures at elementary and cosmic scales, *Kybernetes: The Int. J. Systems & Cybernetics* **32**, no. 7/8, 1005-1020, Eds.: L. Feng, B. P. Gibson and Yi Lin; also arXiv: physics/0301049.

Bounias M. and Krasnoholovets V. (2004). The universe from nothing: A mathematical lattice of empty sets, *Int. J. Anticipatory Computing Systems* **16**, 3-24, Ed.: D. Dubois; arXiv:physics/0309102.

Boyarsky A., Ruchayskiy O. and Shaposhnikov M. (2009). The Role of Sterile Neutrinos in Cosmology and Astrophysics, *Ann. Rev. Nuclear and Particle Science* **59**: 191-214; arXiv:0901.0011 [hep-ph].

Boylan-Kolchin M., Besla G., Hernquist L. (2011). Dynamics of the Magellanic Clouds in a Lambda cold dark matter universe, *Month. Not. Royal Astr. Soc.* **414**, no. 2, 1560–1572.

Brooks A. M. Kuhlen M., Zolotov A., Hooper D. (2013). A baryonic solution to the missing satellites problem, *Astrophys. J.* **765**, 22; arXiv:1209.5394 [astro-phys.CO].

CDMS Collaboration. (2011).Results from a low-energy analysis of the CDMS II Germanium data. arXiv:1011.2482 [astro-phys.CO].

Casado J. (2003). A simple cosmological model with decreasing light speed, arXiv:astro-ph/0310178 [astro-ph].

Clowe D., Gonzalez A. and Markevich M. (2004). Weak-lensing mass reconstruction of the interacting cluster 1E 0657-558: Direct evidence for the existence of dark matter, *Astrophys. J.* **604**, 596-603.

COBE satellite. (2009). http://lambda.gsfc.nasa.gov/product/cobe/

Crothers S. J. (2005). On the ramifications of the Schwarzschild space-time metric, *Progress in Physics* **1**, 74-80, http://www.ptep-online.com/index_files/complete/PP-01-2005.pdf.

Crothers S. J. (2010). The black hole, the Big Bang: A cosmology in crisis, Proc. NPA, http://vixra.org/pdf/1103.0047v1.pdf

Crothers S. J. (2011). The black hole catastrophe: A short reply to J. J. Sharples, *Hadronic J.* **34**, 197-224 (2011); also http://vixra.org/pdf/1206.0080v2.pdf.

Crothers S. J. (2012a). Proof of no "black hole" binary in Nova Scorpii, Global Journal of Science Frontier Research Physics and Space Science Volume 12, no. 4 Version 1.0 June 2012; http://vixra.org/pdf/1206.0080v2.pdf.

Crothers S. J. (2012b). General relativity – a theory in crisis, Global Journal of Science Frontier Research Physics and Space Science Volume 12 Issue 4 Version 1.0 June 2012, http://vixra.org/pdf/1207.0018v2.pdf.

Crothers S. J. (2012c). Proof of the invalidity of the black hole and Einstein's field equations http://vixra.org/pdf/1212.0060v1.pdf.

Guy B. (2010). A modified law of gravitation taking account of the relative speeds of moving masses. A preliminary study, http://hal.archives-ouvertes.fr/hal-00472210.

de Broglie L. (1925). Recherches sur la théorie des quanta, *Ann. de Phys*., 10e série, t. **III**, 22-128 (Janvie-Février); translation by A. F. Kracklauer: *On the theory of quanta*, (Lulu.com; Morrisville, NC; 2007).

de Broglie L. (1967). Sur la Dynamique du corps a masse propre variable et la formule de transformation relativiste de la chaleaur, *Comptes Rendus* **264 B**, no. 15, 1173-1175.

de Broglie L. (1986). *Heisenberg's uncertainty relations and the probabilistic interpretation of wave mechanics*, Mir, Moscow, pp. 42-43 (Russian translation).

de Vega H. J., Sánchez N. G. (2011). Warm dark matter in the galaxies: Theoretical and observational progresses. Highlights and conclusions of the Chalonge CIAS Meudon Workshop 2011 Ecole Internationale d'Astrophysique Daniel Chalonge Meudon campus of Observatoire de Paris in the historic Chˆateau, 8-10 June 2011, arXiv:1109.3187 [astro-phys.CO].

de Vega H. J., Moreno O., Moya de Guerra E., Medrano, M. R., and Sánchez N. G. (2013). Role of sterile neutrino warm dark matter in Rhenium and Tritium beta decays, *Nucl. Phys. B* **866**, 177-195.

Einasto J. (2010). Dark matter, in *Astronomy and Astrophysics*, Eds.: O. Engvold, J. Lattanzio, B. Czerny and R. Stabell, The EOLSS On-line is a virtual library http://www.eolss.net/outlinecomponents/Astronomy-Astrophysics.aspx, arXiv:0901.0632 [astro-ph.CO].

Einstein A. (1916). Die Grundlage der allgemeinen Relativitätstheorie, Annalen der Physik 354, no. 7, 769-822.

Ellis G. and Uzan J. (2003). c is the speed of light, isn't it?, *Am. J. Phys*. **73**, 240-247; arXiv: gr-qc/0305099.

Famaey B. and McGaugh S. (2012). Modified Newtonian dynamics (MOND): Observational phenomenology and relativistic extensions, arXiv:1112.3960 [astro-ph.CO].

Famaey B. and McGaugh S. (2013). Challenges for ΛCDM and MOND, arXiv:1301.0623 [astro-ph.CO].

Feng J. I. and Kumar J. (2008). The WIMPless miracle: Dark matter particles without weak-scale masses or weak interactions, *Phys. Rev. Lett*. **101**, 231301, 4 pages; arXiv:0803.4196 [hep-ph].

Feng J. Q., Gallo C.F. (2008). Galactic rotation described with various thin-disk gravitational models. arXiv:0804.0217 [astro-ph].

Feng J. Q., Gallo C.F. (2011). Modeling the Newtonian dynamics for rotation curve analysis of thin-disk galaxies, Res. Astronomy and Astrophysics, 11, no. 12, 1429-1448.

Fort B. and Mellier Y. (1994). Arc(let)s in clusters of galaxies, *Astronomy and Astrophys. Rev*. **5**, 239-292.

Freedman W. L. (2000). Determination of cosmological parameters, *Phys. Scripta* **85**, 37-46; arXiv:astro-ph/9905222.

Friedmann A. (1922). Über die Krümmung des Raumes, *Zeitschrift für Physik A* **10** (1): 377–386.

Garret K. and Dūda G. (2011). Dark matter: A primer, *Advances in Astronomy*, Volume 2011, Article ID 968283, 22 pages.

Ghosh P. P., Mukhopadhyay U. and Ray S. (2012). Does accelerating Universe permit varying speed of light? *Astrophys. Space Sci.* **337**, no. 2, 509-510.

Gilmore G., Wilkinson M. I., Wyse R. F. G., Kleyna J. T., Koch A., Evans N. W., Grebel E. K., (2007).The observed properties of dark matter on small spatial scales, *Astrophys. J.* **663**, 948-959.

Hajdukovic, D. S. (2011). Is dark matter an illusion created by the gravitational polarization of the quantum vacuum?, *Astrophys. Space Sci.* **334**, 215-218; arXiv:1106.0847 [physics.gen-ph].

Hofer W. A. (2012). Heisenberg, uncertainty, and the scanning tunneling microscope, *Frontiers of Physics* **7**, 218-222; arXiv:1105.3914.

Hoyle, F.; Burbidge, G.; Narlikar, J. V. (1993). A quasi-steady state cosmological model with creation of matter, *Astrophys. J.* **410**, 437–457.

Hoyle, F.; Burbidge, G.; Narlikar, J. V. (1994). Further astrophysical quantities expected in a quasi-steady state Universe, *Astronomy Astrophys*. **289**, no. 3, 729–739.

Hubble E. (1929). A relation between distance and radial velocity among extra-galactic nebula, *Proc. Nat. Acad. Scien.* **15,** no. 3, 168-173.

Jee M. J., Ford H. C., Illingworth G. D., White R. L., Broadhurst T. J., Coe D. A., Meurer G. R., van der Wela, Benítez N., Blakeslee J. P., Bouwens R. J., Bradley L. D., Demarco R., Homeier N. L., Martel A. R., and Mei

S. (2007). Discovery of a ringlike dark matter structure in the core of the galaxy cluster Cl 0024+17, *Astrophys. J*. **661**, 728-749.
Kamada A., Yoshida N., Kohri K., Takahashi T. (2013). Structure of dark matter halos in warm dark matter models and in models with long-lived charged massive particles, arXiv:1301.2744 [astro-phys.CO].
Kozyrev N. A. (1977). Astronomical observations by means of the physical properties of time, in: *Flaring Stars: Proceedings of the Symposium dedicated to the openeing 2.6-m telescope of the Byurakan Astrophysical Observatory*, Byurakan, October 5-8, 1976. Yerevan, pp. 209-227; in Russian.
Kozyrev N. A. and Nasonov V. V. (1978). A new method of determination of trigonometric parallaxes on the basis of measurements of difference between apparent and visible position of stars, in: *Asronometry and Celestial Mechanics*, Akademiya Nauk SSSR, Moscow, Leningrad, pp. 168-179.
Krasinsky G. A. and Brumberg G.A. (2004). Secular increase of astronomical unit from analysis of the major planets motions, and its interpretation. *Celest. Mech. & Dyn. Astron.*, **90**, 267.
Krasnoholovets V. (1997). Motion of a relativistic particle and the vacuum, *Phys. Essays* **10**, no. 3, 407-416; arXiv:quant-ph/9903077.
Krasnoholovets V. (2001a). On the theory of the anomalous photoelectric effect stemming from a substructure of matter waves, *Ind. J. Theor. Phys.* **49,** no. 1, 1-32; arXiv:quant-ph/9906091.
Krasnoholovets V. (2001b). On the mass of elementary carriers of gravitational interaction, *Spacetime & Substance* **2**, no. 4, 169-170; arXiv:quant-ph/0201131.
Krasnoholovets V. (2002). Submicroscopic deterministic quantum mechanics, *Int. J. Computing Anticipatory Systems* **11**, 164-179; arXiv:quant-ph/0109012.
Krasnoholovets V. (2003). On the nature of the electric charge, *Hadronic J. Suppl.* **18**, no. 4, 425-456; arXiv.org:physics/0501132.
Krasnoholovets V. (2008). Reasons for the gravitational mass and the problem of quantum gravity. In *Ether space-time and cosmology*, Vol. 1; Duffy M., Levy J. and Krasnoholovets V., Eds.; PD Publications: Liverpool, pp. 419-450; arXiv:1104.5270 [physics.gen-ph].
Krasnoholovets V. (2009). On microscopic interpretation of phenomena predicted by the formalism of general relativity, in *Ether space-time and cosmology*, Vol. 2: *New insights into a key physical medium*. Eds.: Duffy M. C. and Lévy J. (Apeiron, 2009), pp. 417-431 [Totally 488 pages. Publisher: C. Roy Keys Inc. (Apeiron); also in *Apeiron* **16**, no. 3, 418-438 http://redshift.vif.com/JournalFiles/V16NO3PDF/V16N3KRA.pdf.
Krasnoholovets V. (2010). Inerton fields: Very new ideas on fundamental physics, *American Inst. Phys. Conf. Proc.* - December 22, Vol. 1316, 244-268. Search for fundamental theory: The VII international symposium honoring French mathematical physicist Jean-Pierre Vigier (12-14 July 2010, Imperial College, London), Eds.: R. L. Amoroso, P. Rowlands and S. Jeffers.
Krasnoholovets V. (2011). Dark matter as seen from the physical point of view, *Astrophys. Space Sci.* **335**, no. 2, 619-627.
Krasnoholovets V. (2013a). Inerton field effects in nanosystems, in *Research Horizons of Nanosystems: Structure, Properties and Interactions*, Ed.: M. Putz, Apple Academy Press and CRC Press, Taylor & Francis Group, in press.
Krasnoholovets V. (2013b). On the gravitational time delay effect and the curvature of space, *Int. J. Computing Anticipatory Systems*, in press.
Krasnoholovets V. and Byckov V. (2000). Real inertons against hypothetical gravitons. Experimental proof of the existence of inertons, *Ind. J. Theor. Phys.* **48**, no. 1, 1-23; arXiv.org:quant-ph/0007027.
Krasnoholovets V. and Ivanovsky D. (1993). Motion of a particle and the vacuum, *Phys. Essays* **6**, no. 4, 554-563; arXiv:quant-ph/9910023.
Krasnoholovets V., Skliarenko S. and Strokach O. (2006). On the behavior of physical parameters of aqueous solutions affected by the inerton field of Teslar technology, *Int. J. Mod. Phys. B* **20**, no. 1, 111-124; arxiv:0810.2005 [physics.gen-ph].
Krasnoholovets V., Kukhtarev N. and Kukhtareva T. (2006). Heavy electrons: Electron droplets generated by photogalvanic and pyroelectric effects, *Int. J. Mod. Phys. B* **20**, no. 16, 2323-2337; arXiv:0911.2361 [quant-ph].
Krasnoholovets V. and Lev B. (2003). Systems of particles with interaction and the cluster formation in condensed matter, *Cond. Matt. Phys*. **6**, 67-83; arXiv:cond-mat/0210131.
Kroupa, P. (2012). The dark matter crisis: Falsification of the current standard model of cosmology. *Publications of the Astronomical Society of Australia* **29,** no. 4, 395-433; arXiv:1204.2546 [astro-ph.CO].
Kroupa P., Pawlowski M., Milgrom M. (2012) The failures of the standard model of cosmology require a new paradigm. *Int. J. Mod. Phys. D* **21**, 1230003 [13 pages]; arXiv:1301.3907 [astro-ph.CO].
Lavrentiev M. M., Yeganova I. E., Lutset M. K. and Fominykh S. F. (1990). About distant influence of stars on a resistor. *Proceed. Acad. Scien. USSR* **314**, no. 2, 352-355; in Russian.
Lavrentiev M. M., Gusev V. A., Yeganova I. A., Lutset M. K. and Fominykh S. F. (1990). About the registration of an actual position of the Sun, *Proc. Acad. Sci. USSR* **315**, no. 2, 368–370; in Russian.

Lämmerzahl C., Preuss O., and Dittus H. (2008). Is the physics within the Solar system really understood? arXiv:gr-qc/0604052.
Lemaître G. (1931). Expansion of the universe. A homogeneous universe of constant mass and increasing radius accounting for the radial velocity of extra-galactic nebulæ, *Mon. Not. R. Astron. Soc.* **91**, 483–490.
Loinger A. (2002). *On black holes and gravitational waves* (La Goliardica Pavese).
Loinger A. (2007). *More on BH's and GW's*. III (La Goliardica Pavese).
Magueijo J. (2003). New varying speed of light theories, *Rep. Progr. Phys.* **66**, 2025-2068 (2003), arXiv:astro-ph/0305457.
Mannheim P. D. and O'Brien J. G. (2010). Fitting galactic rotation curves with conformal gravity and a global quadratic potential, Arxiv:1011.3495 [astro-ph.CO].
Mannheim P. D. and O'Brien J. G. (2011). Impact of a global quadratic potential on galactic rotation curves, *Phys. Rev. Lett*. **106**, no. 12, 121101.
McCulloch M. E. (2012). Testing quantised inertia on galactic scales, arXiv:1207.7007 [physics.gen-ph].
Merritt D. and Bertone, G. (2005). Dark matter dynamics and indirect detection. *Mod. Phys. Lett. A* **20**, no. 14, 1021–1036.
Milgrom M. (1983). A modi_cation of the Newtonian dynamics as a possible alternative to the hidden mass hypothesis, *Astrophys. J.* **270**, 365-370.
Milgrom A. (2009). The MOND limit from space-time scale invariance, *Astrophys. J.* **698**, 1630-1639; arXiv: 0810.4065 [astro-phys.].
Nesbet R. K. (2013). Conformal gravity: Dark matter and dark energy, *Entropy* **15**, 162-176.
Penzias A. A. and Wilson R. W. (1965). A measurement of excess antenna temperature at 4080 Mc/s, *Astrophys. J.* **142**, 419–421.
Perlmutter S., Aldering G., Goldhaber G., Knop R. A., Nugent P., Castro P. G., Deustua S., Fabbro S., Goobar A., Groom D. E., Hook I. M., Kim A. G., Kim M. Y., Lee J. C., Nunes N. J., Pain R., Pennypacker C. R., Quimby R., Lidman C., Ellis R. S., Irwin M., McMahon R. G., Ruiz-Lapuente P., Walton N., Schaefer B., Boyle B. J., Filippenko A. V., Matheson T., Fruchter A. S., Panagia N., Newberg H. J. M., Couch W. J. (The Supernova Cosmology Project). (1999). Measurements of Ω and Λ from 42 high-redshift supernovae, *Astrophys. J.* **517**, no. 2, 565-586; arXiv:astro-ph/9812133.
Petit J. P. and d'Agostini G. (2007). Bigravity: a bimetric model of the Universe with variable constants, including VSL (variable speed of light), arXiv:0803.1362 [physics.gen-ph].
Poncaré H. (1906) Sur la dynamique de l'électron, *Rendiconti del Circolo matematico di Palermo* **21**, 129-176; also: Oeuvres, t. IX, pp. 494-550 (in Russian translation: *Selected Transactions*, ed. N. N. Bogolubov (Nauka, Moscow, 1974), **3**, 429-486).
Rabounski D. (2008). On the current situation concerning the black hole problem. *Progress in Physics* **1**, 101–103.
Robertson H. P. (1935). Kinematics and world structure, *Astrophys. J.* **82**, 284–301.
Robitaille P.-M. (2007). WMAP: A radiological analysis, *Progress in Physics* **1**, no. 1, 3-18.
Robitaille P.-M. (2009). COBE: A radiological analysis, *Progress in Physics* **4**, no. 1, 17-42.
Robitaille P.-M. (2010a). Calibration of microwave reference blackbodies and targets for use in satellite observations: An analysis of errors in theoretical outlooks and testing procedures *Progress in Physics*, **3**, no. 1, 3-10.
Robitaille P.-M. (2010b). The Planck satellite LFI and the microwave background: importance of the 4K reference targets, *Progress in Physics* **3**, no. 1, 11-18.
Rocha G., Contaldi C. R., Colombo L. P. L., Bond J. R., Gorski K. M., and Lawrence C. R. (2010). Application of XFASTER power spectrum and likelihood estimator to Planck, *Mon. Not. R. Astron. Soc.* **414**, 823-846; arXiv:1008.4948 [astro-ph.CO].
Rocha M., Peter A. H. G., Bullock J. S., Kaplinghat M., Garrison-Kimmel S., Oorbe J., and Moustakas L. A. (2012). Cosmological simulations with self-interacting dark matter I: Constant density cores and substructure, arXiv:1208.3025 [astro-ph.CO].
Salih M. A., Tomsah I. B. I., Al Mahdi T. M. (2012). General relativity in microscopic scale (GRMS), *J. Basic. Appl. Sci. Res.* **2**, no. 12, 12348-12353.
Santilli R. M. (2006). *Isodual theory of antimatter with applications to antigravity, grand unification, and cosmology*, Kluwer Academic Publishers, Boston, Dordrecht, London, pp. 25-28, 187.
Schmidt B. P., Suntzeff N. B., Phillips M. M., Schommer R. A., Clocchiatti A., Kirshner R. P., Garnavich P., Challis P., Leibundgut B., Spyromilio J., Riess A. G., Filippenko A. V., Hamuy M., Smith R. C., Hogan C., Stubbs C., Diercks A., Reiss D., Gilliland R., Tonry J., Maza J., Dressler A., Walsh J., Ciardullo R. (1998). The high-z supernova search: Measuring cosmic deceleration and global curvature of the universe using type IA supernovae, *Astrophys. J.* **507**, no. 1, 46-63; arXiv:astro-ph/9805200.
Schwarzschild K. (1916). Uber das Gravitationsfeld eines Massenpunktes nach der Einsteinschen Theorie. *Sitzungsberichte der Kniglich Preussischen Akademie der Wissenschaften* **1**, 189-196.

Shnol S. E. (2001). Macroscopic fluctuations are possible consequences of fluctuations of space-time. Arithmetical and cosmological physical aspects, *Rossiyskiy Khimicheski Zhurnal* **65**, no. 1, 12-15.

Shnoll S. E. (2009). *Cosmophysical factors in random processes*, Svenska fysikarkivet, Täby (in Russian). Second edition, supplemented: (2012) American Research Press, Rehoboth, New Mexico, USA.

Shnoll S. E., Rubinshtejn I. A., Zenchenko K. I., Shlekhtarev V. A, Kaminsky A. V., Konradov A. A., and Udaltsova N. V. (2005). Experiments with rotating collimators cutting out pencil of α-particles at radioactive decay of 239Pu evidence sharp anisotropy of space, *Progr. Phys.* vol. **1**, 81–84; arXiv:physics/0501004 [physics.space-ph].

Shnol S. E., Zenchenko T. A., Zenchenko K. I., Pozharski E. V., Kolombet V. A. and Konradov A. A. (2000). Regular changes of fine structure of statistical distributions as a consequence of cosmological physical factors, *Uspekhi Fiz. Nauk* **170**, no. 2, 214-218.

Stasielak J., Biermann P. L., and Kusenko A. (2006). Thermal evolution of the primordial clouds in warm dark matter models with keV sterile neutrinos, arXiv: astro-ph/0606435.

The Top 30 Problems with the Big Bang. (2002). *Apeiron* **9**, no. 2, 72-90. http://redshift.vif.com/JournalFiles/V09NO2PDF/V09N2tvf.PDF.

Thornhill C. K. (2001). A non-singular ethereal cosmology, *Hadronic J. Suppl.* **16**, 203-262.

Tinker J., Kravtsov A. V., Klypin A., Abazajian K., Warren M., Yepes G., Gottlöber S., Holz D. E. (2008). Toward a halo mass function for precision cosmology: the limits of universality, *Astrophys. J.* **688**, 709-728.

Toffolatti L., Burigana C., Argüeso F., and Diego J. M. (2012). Extragalactic compact sources in the Planck sky and their cosmological implications, in *Open Questions in Cosmology*, G. J. Olmo (Ed.), (IFIC - Spain) and published by InTechOpen, Chapter 3, p. 57-86 (2012); arXiv:1302.3355 [astro-phys.CO].

Turyshev S. G., Toth V. T., Kinsella G., Lee S.-C., Lok S. M. and Ellis J. (2012). Support for the thermal origin of the Pioneer anomaly, *Phys. Rev. Lett.* **108**, 241101 (5 pages); arXiv:1204.2507 [gr-qc].

Turyshev S. G., Toth V. T. and Sazhin M. V. (2013). General relativistic observables of the GRAIL mission, *Phys.Rev.* **D87** 024020 (29 p.); arXiv:1212.0232 [gr-qc].

Van Dyck R. S., Jr., Ekstrom P., and Dehmelt H G. (1976). Axial, magnetron, cyclotron and spincyclotron beat frequencies measured on single electron almost at rest in free space (Geonium), *Nature* **262**, 776–777.

Van Dyck R. S., Jr., Schwinberg P. B. and Dehmelt H. G. (1986). Electron magnetic moment from geonium spectra: Early experiments and background concepts. *Phys. Rev. D* **34**, 722–736.

Volovik, G. (2003). *The universe in a Helium droplet*, Clarendon Press, Oxford.

Walker, A. G. (1937). On Milne's theory of world-structure, *Proc. London Math. Soc.* S2-**42**, no. 1, 90–127.

Wilczek F. (2009). What is space? *Physics @MIT* 30, http://web.mit.edu/physics/people/faculty/docs/wilczek_space06.pdf.

WMAP satellite. Tests of Big Bang: The CMB. (2011). http://map.gsfc.nasa.gov/universe/bb_tests_cmb.html.

Zolotov A., Brooks A. M., Willman B., Governato F., Pontzen A., Christensen C., Dekel A., Quinn T., Shen S., and Wadsley J. (2012). *Astrophys. J.* **761,** 71; arXiv:1207.0007 [astro-phys.CO].